YANKEE ATOMIC ELECTRIC COMPANY

YANKEE

YANKEE ATOMIC ELECTRIC COMPANY

YANKEE

6

YAEC-1752

STAR METHODOLOGY APPLICATION
FOR PWR'S
CONTROL ROD EJECTION
MAIN STEAM LINE BREAK

VOLUME 1

CODE DESCRIPTION
BENCHMARKS

September 1990

Major Contributors:

N. Fujita
D. A. Rice
M. W. Scott
R. J. Weader

Yankee Atomic Electric Company
Nuclear Services Division
580 Main Street
Bolton, Massachusetts 01740

Prepared by: N. Fujita 9/20/90

N. Fujita, Senior Engineer (Date)
Transient Analysis Group

Prepared by: David A. Rice 9/20/90

D. Rice, Nuclear Engineer (Date)
Transient Analysis Group

Prepared by: Michael W. Scott 9/20/90

M. W. Scott, Senior Nuclear Engineer (Date)
Nuclear Engineering Department

Prepared by: Richard J. Weader II 9/20/90

R. J. Weader, Principal Engineer (Date)
Reactor Physics Group

Reviewed/ Approved by: P. A. Bergeron 9/20/90

P. A. Bergeron, Manager (Date)
Transient Analysis Group

Reviewed/ Approved by: R. J. Cacciapouti 9/20/90

R. J. Cacciapouti, Manager (Date)
Reactor Physics Group

Approved by: Bruce C. Slifer 9/20/90

B. C. Slifer, Director (Date)
Nuclear Engineering Department

DISCLAIMER OF RESPONSIBILITY

This document was prepared by Yankee Atomic Electric Company for its own use and distribution and on behalf of Maine Yankee Atomic Power Corporation, Vermont Yankee Nuclear Power Corporation, New Hampshire Yankee, and the joint owners of the Seabrook Nuclear Power Station. This document is believed to be completely true and accurate to the best of our knowledge and information.

This document describes the computer code called STAR which is a proprietary software product of Yankee Atomic Electric Company.

Many of the intended uses of STAR have been extensively tested and found to be performing satisfactorily. However, not every possible use of STAR can be anticipated and therefore Yankee Atomic Electric Company, Maine Yankee Atomic Power Corporation, Vermont Yankee Nuclear Power Corporation, New Hampshire Yankee, and the joint owners of the Seabrook Nuclear Power Station and their officers, directors, agents, and employees assume no liability NOR MAKE ANY WARRANTY OR REPRESENTATION OF ANY KIND, WHETHER STATUTORY, WRITTEN, ORAL, OR IMPLIED (INCLUDING WARRANTIES OF FITNESS FOR A PARTICULAR PURPOSE AND MERCHANTABILITY), with respect to the contents of this document or to its accuracy or completeness, or with respect to the contents of the code or to the accuracy or correctness of the calculations performed by the STAR code.

ABSTRACT

This report presents a description of the Space and Time Analysis of Reactors (STAR) computer code and its application to the Rod Ejection and Main Steam Line Break transients. Volume 1 of the report provides the history and theory of the STAR code including both static and transient theory. Volume 1 also includes the code benchmarks with classic numeric cases, Combustion Engineering's HERMITE computer code, and an actual rod drop transient that occurred at Rowe. Volume 2 contains a description of the use of STAR in methodology for the Rod Ejection and Main Steam Line Break transients. Current licensing methods are described to illustrate how the STAR application for each transient is an extension of the current approved method. A demonstration analysis is included for each transient application.

TABLE OF CONTENTS

LIST OF TABLES

LIST OF FIGURES

LIST OF FIGURES
(Continued)

LIST OF FIGURES
(Continued)

1.0 INTRODUCTION

This report provides a description of the Space and Time Analysis of Reactors (STAR) computer program, code benchmarks, and applications to the Control Rod Ejection and Main Steam Line Break transients. The STAR based methodology is an extension of the current approved methods used by Yankee Atomic Electric Company (YAEC) for analysis of these transients.

YAEC currently uses a point kinetics approach CHIC-KIN[1], to perform the rod ejection analysis. The present methodology[2] also includes an option to utilize bounding radial Doppler weighting factors[3] generated by Combustion Engineering's HERMITE computer code to simulate the spatial reactivity feedback effects in the point kinetics scheme. The NRC has approved this methodology for application to Maine Yankee[4]. The proposed method described in Volume 2 is the same, except the STAR computer program would replace HERMITE in the generation of Doppler weighting factors and would allow similar factors to be developed for other PWR's.

For the steam line break YAEC currently uses RETRAN-02 and the Boron Injection RETRAN Post-Processor (BIRP) code[5,6]. RETRAN is used to conservatively predict the thermal-hydraulic conditions following the steam line break while BIRP computes the overall reactivity to determine whether or not return to power occurs. The current YAEC methodology is limited to no return to power due to the lack of a method to account for spatial effects on moderator feedback. The main steam line break methodology was approved by the NRC[7]. The proposed method described in Volume 2 uses the STAR code to account for spatial effects and allow the treatment of return to power. In addition this method uses a later version of RETRAN, RETRAN-02 MOD 05, which contains a boron transport model that allows for the elimination of the BIRP post processor code to treat boron injection. Therefore, the new method would use RETRAN point kinetics to predict the power response and the STAR code to account for spatial effects on moderator feedback. RETRAN results are demonstrated as conservative by comparison with STAR.

2.0 STAR CODE DESCRIPTION

2.1 STAR History

The STAR code, which is based on the analytic nodal method of the QUANDRY computer code[8], was developed jointly by NUS Corporation and YAEC from the early 1980's through May of 1987. NUS withdrew from the development effort in May of 1987 and YAEC continued with the effort to date. Since May of 1987, YAEC has added thermal-hydraulic methods to the code and SIMULATE-3 cross section processing.

2.2 STAR Theory

The STAR code solves the three dimensional space dependent reactor static and transient neutronic problem with thermal-hydraulic feedback. In performing this function, STAR utilizes the analytic nodal method formalism with a quadratic transverse leakage approximation[8,9] and discontinuity factors[10,11]. STAR performs its global flux solution using a standard center mesh coarse mesh finite difference (CMFD) scheme like the CITATION code[12]. Discontinuity factors obtained from the QUANDRY equations are used to force agreement between the CMFD solution and the QUANDRY solution. A nonlinear iteration process is used in the solution. The derivation and formulation of the STAR equations and logic is presented in this section. The text is predominantly extracted from Reference (8).

2.2.1 Formulation of The Analytic Nodal Diffusion Equations

In the multigroup diffusion theory approximation, the set of time and space dependent coupled partial differential equations for which the approximate solutions are sought can be written in a matrix form with brackets denoting the matrices as

$$\begin{aligned}\underline{\nabla} \cdot [D(\underline{r},t)]\, \underline{\nabla}\, [\phi(\underline{r},t)] - [\Sigma_T(\underline{r},t)][\phi(\underline{r},t)] \\ + (1-\beta)[\chi_p][\frac{1}{\lambda}\, \nu\Sigma_f(\underline{r},t)]^T\, [\phi(\underline{r},t)] \\ + \sum_{d=1}^{D} \lambda_d[\chi_d]C_d(\underline{r},t) = [v]^{-1}\, \frac{\partial}{\partial t}[\phi(\underline{r},t)]\end{aligned} \qquad \text{(2-1a)}$$

$$\beta_d[\frac{1}{\lambda}\, \nu\Sigma_f(\underline{r},t)]^T\, [\phi(\underline{r},t)] - \lambda_d C_d(\underline{r},t) = \frac{\partial}{\partial t}C_d(\underline{r},t)\ ;\ d = 1, 2 \ldots D \qquad \text{(2-1b)}$$

where the notation is standard except that the matrix $[\Sigma_T(\underline{r},t)]$ contains the macroscopic total cross section minus scattering cross sections and β represents the total delayed neutron fraction, while β_d represents the delayed neutron fraction for each delayed neutron group.

The rigorous nodal balance equations are derived by integrating Equation 2-1 over the volume of an arbitrary 3-D Cartesian node (i,j,k) with x, y, and z dimensions h_x, h_y, and h_z to obtain

$$\begin{aligned}- h_y^j h_z^k([J_{x_{i,j,k}}(t)] - [J_{x_{i,j,k}}(t)]) - h_x^i h_z^k([J_{y_{i,j+1,k}}(t)] - [J_{y_{i,j,k}}(t)]) \\ - h_x^i h_y^j([J_{z_{i,j,k+1}}(t)] - [J_{z_{i,j,k}}(t)]) - V_{i,j,k}[\Sigma_{T_{i,j,k}}(t)][\overline{\phi_{i,j,k}}(t)] \\ + (1-\beta)V_{i,j,k}[\chi_p][\frac{1}{\lambda}\, \nu\Sigma_{f_{i,j,k}}]^T\, [\overline{\phi_{i,j,k}}(t)] + \sum_{d=1}^{D}\lambda_d V_{i,j,k}[\chi_d]\overline{C_{d_{i,j,k}}}(t) \\ = V_{i,j,k}[v]^{-1}\frac{\partial}{\partial t}[\overline{\phi_{i,j,k}}(t)]\end{aligned} \qquad \text{(2-2a)}$$

$$\beta_d\left[\frac{1}{\lambda}\nu\Sigma_{f_{i,j,k}}(t)\right]^T[\overline{\phi_{i,j,k}}(t)] - \lambda_d\overline{C_{d_{i,j,k}}}(t) = \frac{\partial}{\partial t}\overline{C_{d_{i,j,k}}}(t)\ ;\ d = 1,\ 2\ \ldots\ D \tag{2-2b}$$

where

$$[J_{x_{i,j,k}}(t)] \equiv -\frac{1}{h_x^i h_z^k}[D_{i,j,k}]\frac{\partial}{\partial x}\int_{y_j}^{y_{j+1}}dy\int_{z_k}^{z_{k+1}}dz[\phi(x,y,z,t)]$$

$$[\overline{\phi_{i,j,k}}(t)] \equiv \frac{1}{h_x^i h_y^j h_z^k}\int_{x_i}^{x_{i+1}}dx\int_{y_j}^{y_{j+1}}dy\int_{z_k}^{z_{k+1}}dz[\phi(x,y,z,t)]$$

$$\overline{C_{d_{i,j,k}}}(t) \equiv \frac{1}{h_x^i h_y^j h_z^k}\int_{x_i}^{x_{i+1}}dx\int_{y_j}^{y_{j+1}}dy\int_{z_k}^{z_{k+1}}dz\ C_d(x,y,z,t)$$

$$V_{i,j,k} \equiv h_x^i h_y^j h_z^k$$

T utility of Equation 2-2 is limited by the fact that without additional relationships between node-averaged fluxes and face-averaged currents, the spati flux distribution cannot be determined.

One method of obtaining a differential equation from which this spatial coupling can be determined is to treat the directions one at a time by spatially integrating Equation 2-1 over the two directions transverse to the direction of interest. For example, consider the x direction in node (i,j,k) for which the following expression is obtained:

$$
\begin{aligned}
&- [D_{i,j,k}(t)]\frac{\partial^2}{\partial x^2}[\phi_{x_{i,j,k}}(x,t)] \\
&- \frac{1}{h_y^j h_z^k}[D_{i,j,k}(t)]\int_{y_j}^{y_{j+1}} dy \int_{z_k}^{z_{k+1}} dz\ \frac{\partial^2}{\partial y^2}[\phi(x,y,z,t)] \\
&- \frac{1}{h_y^j h_z^k}[D_{i,j,k}(t)]\int_{y_j}^{y_{j+1}} dy \int_{z_k}^{z_{k+1}} dz\ \frac{\partial^2}{\partial z^2}[\phi(x,y,z,t)] \qquad (2\text{-}3) \\
&+ \{[\Sigma_{T_{i,j,k}}(t)]\ [\omega_{p_{i,j,k}}(t)][v]^{-1} \\
&- ((1-\beta)[\chi_p] + \sum_{d=1}^{D}\frac{\lambda_d\beta_d}{(\omega_{d_{i,j,k}}(t)+\lambda_d)}[\chi_d])[\frac{1}{\lambda}\ \nu\Sigma_{f_{i,j,k}}(t)]^T\}[\phi_{x_{i,j,k}}(x,t)] \\
&= 0
\end{aligned}
$$

where

$$
[\phi_{x_{i,j,k}}(x,t)] \equiv \frac{1}{h_y^j h_z^k}\int_{y_j}^{y_{j+1}} dy \int_{z_k}^{z_{k+1}} dz\ [\phi(x,y,z,t)]
$$

and the approximation

$$
\begin{aligned}
\frac{\partial}{\partial t}[\phi_{x_{i,j,k}}(x,t)] &= [\omega_{d_{i,j,k}}(t)][\phi_{x_{i,j,k}}(x,t)] \\
\frac{\partial}{\partial t}C_{d_{i,j,k}}(x,t) &= \omega_{d_{i,j,k}}(t)\ C_{d_{i,j,k}}(x,t)
\end{aligned}
$$

has been made.

A y-directed net leakage, L_y, as a function of x can be defined as

$$h_z^k[L_{y_{i,j,k}}(x,t)] \equiv -[D_{i,j,k}] \int_{y_j}^{y_{j+1}} dy \int_{z_k}^{z_{k+1}} dz \ \frac{\partial^2}{\partial y^2}[\phi(x,y,z,t)]$$

This leakage possesses the property that when integrated over $[x_i, x_{i+1}]$ and divided by h_x^i yields

$$\frac{1}{h_x^i}\int_{x_i}^{x_{i+1}} dx[L_{y_{i,j,k}}(x,t)] = [J_{y_{i,j+1,k}}(t)] - [J_{y_{i,j,k}}(t)] \equiv [\overline{L_{y_{i,j,k}}}(t)]$$

which is the nodal faced-averaged, y-directed, net leakage. By defining a sum of leakages transverse to the x direction, S_x, as

$$[S_{x_{i,j,k}}(x,t)] \equiv \frac{1}{h_y^j}[L_{y_{i,j,k}}(x,t)] + \frac{1}{h_z^k}[L_{z_{i,j,k}}(x,t)]$$

Equation 2-3 can be expressed as

$$\begin{aligned}
&-[D_{i,j,k}] \frac{\partial^2}{\partial x^2}[\phi_{x_{i,j,k}}(x,t)] + \{[\Sigma_{T_{i,j,k}}(t)] + [\omega_{p_{i,j,k}}(t)][v]^{-1} \\
&- ((\frac{1}{\beta})[\chi_p] + \sum_{d=1}^{D} \frac{\lambda_d \beta_d}{(\omega_{d_{i,j,k}}(t)+\lambda_d)}[\chi_d])[\frac{1}{\lambda}\nu\Sigma_{f_{i,j,k}}(t)]^T\}[\phi_{x_{i,j,k}}(x,t)] \\
&= -[S_{x_{i,j,k}}(x,t)]
\end{aligned} \tag{2-4}$$

To obtain relationships between the node-averaged fluxes and the face-averaged net leakages, one need only solve Equation 2-4 for $[\phi_{xi,j,k}(x,t)]$ (and the analogous equations for the y and z directions) and integrate this "one dimensional" flux over the node. Unfortunately, the x-dependence of the transverse leakage source on the right hand side of Equation 2-4 must be known or approximated if the solution is to be found. This circumstance makes necessary the first, and only, spatial approximation in the analytic nodal method.

Finneman[18] has suggested a method for employing quadratic polynomials in order to determine uniquely the shape of the transverse leakage in a node in terms of the average transverse leakages in three adjacent nodes. This approximation leads to a functional form of the y-directed net leakage as a function of x given by

$$\begin{aligned}[L_{y_{i,j,k}}(x,t)] = [\overline{L_{y_{i-1,j,k}}}(t)]\rho_{x_i}^{i-1}(x) &+ [\overline{L_{y_{i,j,k}}}(t)]\rho_{x_i}^{i}(x) \\ &+ [\overline{L_{y_{i+1,j,k}}}(t)]\rho_{x_i}^{i+1}(x)\end{aligned} \tag{2-5}$$

where each of the ρ's is a quadratic polynomial in x. The constraints imposed on the expansion functions, stated physically, are that the integrals of the transverse leakage approximation over each of the three adjacent nodes preserve the average transverse leakage of that node. This form of the transverse leakage is particularly useful since it involves only average transverse leakages which are already unknowns in the nodal balance equation, Equation 2-2.

In the original implementation of the analytic nodal method, equations relating the node-averaged fluxes and the face-averaged net leakages are obtained by eliminating the homogenized surface fluxes from the equations, assuming continuity of the homogenized fluxes. The details of this procedure are shown in Appendix 2 of Reference (8). The expressions resulting from this procedure as implemented in QUANDRY give excellent results for problems where the nodes used are truly homogeneous and will duplicate fine mesh diffusion theory solutions exactly in one-dimensional cases with homogeneous nodes. STAR simplifies the calculations required in the QUANDRY solution by using a coarse mesh finite difference (CMFD) scheme for the global flux iteration and forcing the CMFD solution to agree with the QUANDRY solution by the use of CMFD discontinuity factors. These CMFD discontinuity factors are defined as

$$DFCM = \frac{\textit{Heterogeneous Surface Flux QUANDRY Equations}}{\textit{Homogeneous CMFD Surface Flux}}$$

for each face of each node in each group. The DFCM values are used to calculate current coupling coefficients which are in turn used to calculate the flux multipliers for the CMFD flux iteration. The effect of the CMFD discontinuity factors is to force the CMFD solution to match the QUANDRY solution. These are not to be confused with the assembly discontinuity factors input by the user which correct for the heterogeneous nature of real reactor problems.

In real cases, the nodes used by STAR represent heterogeneous fuel assemblies by homogenized parameters obtained by flux-volume weighting. Smith[14] has generalized Koebke's[15] work on this assembly homogenization problem by introducing quantities called discontinuity factors defined by

$$DF = \frac{\textit{Heterogeneous Surface Flu}}{\textit{Homogeneous Surface Flux}}$$

for each node and each direction in each group. Smith has also shown that discontinuity factors can be approximated by the rati s of single-assembly calculation surface fluxes to assembly-averaged fluxes. These discontinuity factors are then known as assembly discontinuity factors and can be input to STAR by the user. These factors have been successfully applied in the LWR analysis code SIMULATE-3[16].

The expressions relating node-averaged fluxes and face-averaged net leakages, F, subject only to the approximation that the leakage shape can be fit by the quadratic polynomial of Equation 2-5 are given by an equation of the form

$$\begin{aligned}[\overline{L_{x_{i,j,k}}}] = {} & [F^{i-1}_{i,j,k}][\overline{\phi_{i-1,j,k}}] + [F_{x_{i,j,k}}][\overline{\phi_{i,j,k}}] + [F^{i+1}_{x_{i,j,k}}][\overline{\phi_{i+1,j,k}}] \\ & + [G^{i-2}_{x_{i,j,k}}][\overline{S_{x_{i-2,j,k}}}] + [G^{i-1}_{i,j,k}][\overline{S_{x_{i-1,j,k}}}] \\ & + [G^{i}_{x_{i,j,k}}][\overline{S_{x_{i,j,k}}}] + [G^{i+1}_{x_{i,j,k}}][\overline{S_{x_{i+1,j,k}}}] \\ & + [G^{i+2}_{x_{i,j,k}}][\overline{S_{x_{i+2,j,k}}}] \end{aligned} \tag{2-6}$$

where each of the matrices is a full G x G matrix.

By combining Equation 2-6 (and the analogous equations for the y and z directions) and the nodal balance equation, the full set of nodal diffusion equations can be expressed as

$$
\begin{bmatrix} [v]^{-1} & [0] & [0] & [0] \\ [0] & [0] & [0] & [0] \\ [0] & [0] & [0] & [0] \\ [0] & [0] & [0] & [0] \end{bmatrix} \frac{d}{dt} \begin{bmatrix} [\bar{\phi}(t)] \\ [\bar{L}_x(t)] \\ [\bar{L}_y(t)] \\ [\bar{L}_z(t)] \end{bmatrix} = \begin{bmatrix} [F] & [G_x] & [G_y] & [G_z] \\ [F_x] & -[I] & [G_{xy}] & [G_{xz}] \\ [F_y] & [G_{yx}] & -[I] & [G_{yz}] \\ [F_z] & [G_{zx}] & [G_{zy}] & -[I] \end{bmatrix} \begin{bmatrix} [\bar{\phi}(t)] \\ [\bar{L}_x(t)] \\ [\bar{L}_y(t)] \\ [\bar{L}_z(t)] \end{bmatrix}
$$

$$
+ \begin{bmatrix} [M] & [0] & [0] & [0] \\ [0] & [0] & [0] & [0] \\ [0] & [0] & [0] & [0] \\ [0] & [0] & [0] & [0] \end{bmatrix} \begin{bmatrix} [\bar{\phi}(t)] \\ [\bar{L}_x(t)] \\ [\bar{L}_y(t)] \\ [\bar{L}_z(t)] \end{bmatrix} + \sum_{d=1}^{D} \begin{bmatrix} [[\chi_d]\lambda_d C_d(t)] \\ [0] \\ [0] \\ [0] \end{bmatrix} \qquad (2\text{-}7)
$$

where the submatrices are N x N, N being the total number of nodes, while each of the elements of the submatrices is G x G, G being the number of neutron groups. [M] represents the block diagonal prompt fission source matrix and [I] represents the identity matrix. All of the $[F_\alpha]$ matrices of Equation 2-7 are block tridiagonal, the $[G_\alpha]$ matrices are block pentadiagonal, and [F] is block septadiagonal.

2.2.2 Static Applications

The static counterpart to the analytic nodal diffusion equations, Equation 2-7 has been applied to the analysis of light water reactors in two groups. This super-matrix equation is a set of linear equations in the four vector unknowns, $[\bar{\phi}]$, $[\bar{L}_x]$, $[\bar{L}_y]$, $[\bar{L}_z]$. Because of the complicated structure of the equations, iterative methods are required to determine the spatial flux distribution.

2.2.2.1 General Iterative Scheme

The static eigenvalue problem can be expressed in terms of the scalar flux ψ as

$$[H]\,[\psi] = \frac{1}{\lambda}\,[P]\,[\psi] \tag{2-8}$$

where

$$[H] \equiv \begin{bmatrix} [F'] & [G_x] & [G_y] & [G_z] \\ [F_x] & -[I] & [G_{xy}] & [G_{xz}] \\ [F_y] & [G_{yx}] & -[I] & [G_{yz}] \\ [F_z] & [G_{zx}] & [G_{zy}] & -[I] \end{bmatrix},\ [P] \equiv \begin{bmatrix} [M'] & [0] & [0] & [0] \\ [0] & [0] & [0] & [0] \\ [0] & [0] & [0] & [0] \\ [0] & [0] & [0] & [0] \end{bmatrix},\ [\psi] \equiv \begin{bmatrix} [\phi] \\ [\overline{L}_x] \\ [\overline{L}_y] \\ [\overline{L}_z] \end{bmatrix}$$

An accelerated fission source iteration is applied to Equation 2-8 to determine the maximum eigenvalue and corresponding eigenvector. The convergence rate of the fission source iteration is increased by employing "eigenvalue shifting" or Wielandt's fractional iteration[17]. That is, Equation 2-8 is modified to obtain

$$\left([H] - \frac{1}{\lambda_s}\,[P]\right)[\psi] = \left(\frac{1}{\lambda} - \frac{1}{\lambda_s}\right)[P][\psi] \tag{2-9}$$

where λ_s is arbitrarily selected but subject to certain restrictions discussed below. It is easily demonstrated that the eigenvector associated with the maximum value of $(1/\lambda - 1/\lambda_s)^{-1}$ is identical to the eigenvector associated with the maximum value of λ, provided λ_e is chosen to be larger in modulus than λ. Naturally, the convergence rate of the fission source iterations is maximized by choosing λ_e to be equal to λ. Unfortunately, this choice makes the matrix $[H - (1/\lambda_e)P]$ truly singular, and hence impossible to invert. For a wide class of 2-group light water reactor problems, a value, $\lambda_e = \lambda + .05$, appears to be near optimal, with respect to total iterative effort.

The iterative scheme used by STAR to solve equation 2-9 is a nonlinear iteration scheme[18] which is summarized as follows:

1. Evaluate cross sections from the current reactor state.
2. The CMFD current coupling coefficients are evaluated from the CMFD discontinuity factors and cross sections.
3. Wielandt's fractional (outer) iteration is employed to determine the eigenvector and eigenvalue. The flux multipliers for the flux iterations are updated at each outer iteration.
4. Flux iterations are performed using the Cyclic Chebyshev Semi-Iterative Method[19]. Before starting the flux iterations the spectral radius of the flux iteration matrix is calculated by the a. priori method suggested by Varga[19].
5. If the nonlinear iteration is not converged, use the QUANDRY equations to generate updated CMFD discontinuity factors and loop back to Step 2.

One very important property of the static nodal diffusion equation and the numerical methods that are employed to solve them is that convergence to the exact solution of the two-group diffusion equations is guaranteed in the limit of infinitely fine mesh spacing. Since the only approximation in the analytic nodal method is in the shape of the transverse leakages, the method is <u>exact</u> in one-dimensional problems for any mesh spacing, provided equivalent homogenized parameters which are spatially flat within each node are available.

2.2.3 <u>Transient Applications</u>

STAR solves the transient nodal diffusion equations by breaking up the transient into time domains, each of which contains one or more time steps. The solution in each time step is as follows:

1. Changes to cross sections and discontinuity factors because of external perturbations (i.e., control movements) are applied.
2. Nodal fluxes are extrapolated exponentially to the end of the present time step.
3. The thermal hydraulic boundary conditions are updated.
4. Coupling coefficients are updated based on the latest cross sections and CMFD discontinuity factors.
5. The right hand side of the flux iteration equation is updated using a fully implicit backward difference and a flux iteration are performed to advance fluxes to the end of the time step.
6. If non-linear iterations were specified for this time step, QUANDRY equations are used to update CMFD discontinuity factors.
7. Update the thermal hydraulic variables.
8. Update the cross sections using the latest thermal hydraulic conditions.
9. Update the precursor concentrations and prompt and delayed neutron frequencies.

The prompt and delayed neutron frequencies (ω's) of Equation 2-4 are calculated for the time step N from the expressions

$$\omega^N_{p_{g_{i,j,k}}} = \frac{1}{t^N - t^{N-1}} \ln\left(\frac{\bar{\phi}^N_{g_{i,j,k}}}{\bar{\phi}^{N-1}_{g_{i,j,k}}}\right)$$
$$\omega^N_{d_{i,j,k}} = \frac{1}{t^N - t^{N-1}} \ln\left(\frac{\bar{C}^N_{d_{i,j,k}}}{\bar{C}^{N-1}_{d_{i,j,k}}}\right) \qquad (2\text{-}10)$$

where t^N is the time at step N.

10. Perform edits, then start next step.

The coupling coefficients used in the flux iterations are dependent on omega as well as the cross sections, and change with each time step. In practice, the changes occur over a long enough time scale that it is not necessary to perform a non-linear iteration at each time step.

In order to incorporate thermal hydraulic feedback effects, STAR incorporates a number of optional thermal hydraulic models. These include the lumped heat capacity model, WIGL[20], the LRA adiabatic feedback model[21], COBRA-IIIC[22], and VIPRE-01[23]. The LRA models are used in some of the numerical benchmark cases. The WIGL model is used in some of the numerical benchmarks and as a closed channel model for rod ejection problems. COBRA-IIIC was used in the development of open channel steam line break models and has been superseded by VIPRE-01, which has been applied to the EPRI HERMITE comparison (a rod ejection) and to steam line break problems.

3.0 STAR BENCHMARKS

This section describes a series of test problems run to validate the STAR Code for use on steady-state and transient physics problems with and without thermal and hydraulic feedback. All these problems use defined sets of cross sections and feedback parameters to remove the effect of differences in cross section generation and hydraulic modeling on the results; and all these problems have also been solved by other methods which serve as reference solutions. The problems used for this test series are the IAEA PWR Benchmark Problem[21], for Tests 1 and 2; the LRA BWR Kinetic Benchmark[22], for Tests 3, 4, and 9; the TWIGL 2D Kinetic Problem[24], for Tests 5 and 6; the LMW LWR Transient Problem[25], for Test 7; and a variation on the LMW problem[8], for Test 8.

A further verification of STAR was performed by duplicating a comparison commissioned by EPRI of their 3D nodal kinetics code, ARROTTA[26] to the Combustion Engineering licensed code, HERMITE[27]. Finally, a comparison to an actual operational event was performed by analyzing a Yankee Rowe rod drop which occurred on February 18th, 1987.

3.1 Classic Numeric Cases

3.1.1 The IAEA Benchmark Problem

This proble[illegible] esents a rather difficult PWR neutronics problem, and is analyzed in its original 3D form from Reference (21) and as a 2D problem representing the midplane of the 3D problem.

Test 1 is the 2D analysis with axial buckling incorporated as a DB-squared term added to the absorption cross sections. The analysis was performed with 20 cm (assembly sized) and 10 cm radial mesh size. Excellent agreement can be seen in the results shown in Figures 3.1.1 and 3.1.2 with the worst assembly power error less than 1% even with the coarse 20 cm mesh.

Test 2 is the full 3D problem with 20 cm radial and axial mesh (Figure 3.1.3) and with 10 cm radial meshes and 20 cm axial fuel mesh and 10 cm axial reflector mesh (Figure 3.1.4). Again, excellent agreement is seen in both cases, with the worst assembly power error less than 1% in the 10 cm mesh case.

The IAEA Benchmark problem shows that the Analytic Nodal Method with assembly discontinuity factors can produce comparable results to fine-mesh methods, with 20 cm mesh spacings corresponding to the usual PWR assembly size and 10 cm mesh spacings corresponding to the 2 *x* 2 mesh per assembly normally used in PWR analysis.

3.1.2 The LRA BWR Kinetic Problem

The problem represents a BWR rod ejection-type problem with only Doppler feedback terminating the excursion.

Test 3 solves the initial condition for the 2D version of the problem, and Figure 3.1.5

shows that excellent agreement is achieved in both eigenvalue and power distribution.

Test 4 solves the 3D transient version of the LRA BWR transient with a very coarse mesh in quarter core geometry. Figures 3.1.6 through 3.1.11 compare radial power distributions as a function of time with a reference solution generated by QUANDRY, while Table 3.1.1 compares some STAR and QUANDRY results for this problem. The radial power agreement is excellent, while the overall power trace follows the shape of the reference solution as shown by Figure 3.1.12. QUANDRY uses a model for the LRA problem which approximates the temperature shape in the nodes to calculate cross sections, which probably accounts for much of the difference between STAR and QUANDRY total powers given the very peaked radial power shapes in these problems.

Test 9 solves the 2D version of the LRA problem. Figures 3.1.13 through 3.1.19 show the excellent agreement of the radial power solutions between STAR and QUANDRY solutions, while Table 3.1.2 shows reasonable agreement with the powers at various times, and Figure 3.1.20 shows that the overall power trace shape agrees well with QUANDRY. Note that in spite of fairly sizeable disagreements in core power at some times in the transients, the peak nodal fuel temperatures at the end of the transient agree to within 3.1% for the 3D case and 0.3% for the 2D case.

3.1.3 The TWIGL 2D Kinetic Problem

This problem is a 2D model of a 160 cm square unreflected seed blanket reactor with two neutron groups and one delay precursor family. Step and ramp positive reactivity insertions are modeled in the corner seed assemblies. Test 5, the step perturbation, gives power results as shown in Table 3.1.3 and Figure 3.1.21. Test 6, the ramp perturbation, gives results as shown in Table 3.1.4 and Figure 3.1.22. The agreement is excellent in both cases within 1% at every step.

3.1.4 The LMW LWR Transient Problem

The LMW LWR transient problem represents a control rod movement in a simplified PWR. Test 7 represents a solution for this problem using a 10 cm axial mesh and 250 ms time steps.

Table 3.1.5 and Figure 3.1.23 show core powers versus time and Figure 3.1.24 shows the radial power distribution at time zero, all compared to reference solutions reported by Smith[8]. STAR assumes cross sections are always homogeneous within nodes, and simple volume average values are used for nodes which are partly rodded. This leads to some oscillations in power due to control rod cusping. Smith also reports the input and several solutions to the LMW problem with thermal-hydraulic feedback added by a WIGL model.

Figure 3.1.25 is a plot of power versus time for Test 8 (Test 7 with feedback added and a 20 cm axial mesh) compared to a solution reported by Smith. There are large variations in power due to the control rod averaging, but the general trend follows Smith's feedback solution.

TABLE 3.1.1

<u>Comparison of STAR and QUANDRY Results for Very Coarse Mesh 3D LRA BWR Problem</u>

	STAR	**QUANDRY**
Time to First Peak (s)	0.91	0.907
Power at First Peak (w/cc)	5277	5739
Time to First Minimum (s)	1.00	0.988
Power at First Minimum (w/cc)	132.4	109.0
Time to Second Peak (s)	1.60	1.44
Power at Second Peak (w/cc)	377	412
Power at t = 3.0 sec. (w/cc)	71.5	71.2
Peak/Average Assembly Power at 3.0 sec.	3.62	3.64
Peak Nodal Fuel Temperature at 3.0 sec. (°K)	4020	4148

TABLE 3.1.2

<u>Comparison of STAR and Fine Mesh Results for 2D LRA BWR Problem</u>

	STAR	REFERENCE
Number of Spatial Mesh Points	121	484
Initial Eigenvalue	0.99641	0.99636
Time to First Peak (s)	1.43	1.436
Power at First Peak (w/cc)	6363	5411
Power at Second Peak (w/cc)	1023	784
Power at t = 3.0 sec. (w/cc)	55.8	96.2
Peak Fuel Temperature at t = 3.0 sec. (°K)	2939	2948

TABLE 3.1.3

Total Power Versus Time for TWIGL 2D Problem
(Step Perturbation)

TIME (SEC)	STAR	REFERENCE	% DIFFERENCE
0.0	1.0	1.0	-
0.1	2.076	2.061	+0.73
0.2	2.076	2.078	-0.10
0.3	2.098	2.095	+0.14
0.4	2.118	2.113	+0.24
0.5	2.132	2.131	+0.05

TABLE 3.1.4

Total Power Versus Time for TWIGL 2D Problem
(Ramp Perturbation)

TIME (SEC)	STAR	REFERENCE	% DIFFERENCE
0.0	1.0	1.0	-
0.1	1.308	1.307	+0.08
0.2	1.955	1.957	-0.10
0.3	2.087	2.074	+0.63
0.4	2.088	2.098	-0.48
0.5	2.115	2.109	+0.28

TABLE 3.1.5

Average Power Density for STAR and Reference
Solution of the LMW LWR Transient Problem

TIME (SEC)	STAR POWER (W/CC)	REFERENCE (W/CC)
0	150	150
5	163.1	169.4
10	198.3	202.0
20	260.4	260.5
30	211.0	209.9
40	122.9	123.9
50	74.6	76.5
60	58.0	58.6

LEGEND

REFERENCE
STAR
% DIFFERENCE

	1	2	3	4	5	6	7	8	9
Y= 9									
Y= 8	.756	.739	.696						
Y= 7	.934	.951	.976	.850	.603				
Y= 6	.935	1.035	1.070	.908	.691	.585 .586 .22			
Y= 5	.610	1.069	1.178	.968	.470 .470 -.19	.686 .691 .76	.597 .603 .97		
Y= 4	1.207	1.312	1.344	1.193 1.192 -.07	.967 .968 .06	.907 .908 .18	.846 .850 .51		
Y= 3	1.446	1.476	1.469 1.466 -.22	1.345 1.344 -.10	1.179 1.178 -.10	1.071 1.070 -.05	.975 .976 .10	.692 .696 .58	
Y= 2	1.303	1.435 1.429 -.43	1.480 1.476 -.26	1.315 1.312 -.23	1.070 1.069 -.07	1.036 1.035 -.11	.950 .951 .03	.736 .739 .42	
Y= 1	.745 .746 .05	1.310 1.303 -.53	1.454 1.446 -.55	1.211 1.207 -.33	.610 .610 -.05	.935 .935 -.01	.934 .934 -.01	.755 .756 .15	

EIGENVALUE - REFERENCE = 1.02958 STANDARD DEVIATION = .354
- STAR = 1.02961 MAX POSITIVE DIFFERENCE = .972
- DIFFERENCE = .00003 MAX NEGATIVE DIFFERENCE = -.550

FIGURE 3.1.1

STAR Test 1 - IAEA 2D PWR Benchmark - 20 CM Mesh
IAEA 2D - 3 1/3 CM Mesh Nodal Reference

LEGEND

REFERENCE
STAR
% DIFFERENCE

	1	2	3	4	5	6	7	8	9
Y= 9									
Y= 8	.755	.736	.692						
	.755	.736	.693						
	-.03	.04	.19						
Y= 7	.934	.950	.975	.846	.597				
	.934	.950	.975	.847	.598				
	-.04	.01	.04	.12	.26				
Y= 6	.935	1.036	1.071	.907	.686	.585			
	.935	1.036	1.070	.907	.686	.586			
	-.07	-.03	-.02	.01	.04	.23			
Y= 5	.610	1.070	1.179	.967	.470	.686	.597		
	.610	1.069	1.179	.967	.471	.686	.598		
	.01	-.06	-.02	-.02	.03	.04	.26		
Y= 4	1.211	1.315	1.345	1.193	.967	.907	.846		
	1.210	1.315	1.344	1.192	.967	.907	.847		
	-.04	-.02	-.06	-.05	-.02	.01	.12		
Y= 3	1.454	1.480	1.469	1.345	1.179	1.071	.975	.692	
	1.453	1.479	1.469	1.344	1.179	1.070	.975	.693	
	-.07	-.02	-.04	-.06	-.02	-.02	.04	.19	
Y= 2	1.310	1.435	1.480	1.315	1.070	1.036	.950	.736	
	1.309	1.435	1.479	1.315	1.069	1.036	.950	.736	
	-.07	-.02	-.02	-.02	-.06	-.03	.01	.04	
Y= 1	.745	1.310	1.454	1.211	.610	.935	.934	.755	
	.745	1.309	1.453	1.210	.610	.935	.934	.755	
	-.01	-.07	-.07	-.04	.01	-.07	-.04	-.03	

EIGENVALUE - REFERENCE = 1.02958 STANDARD DEVIATION = .084
- STAR = 1.02961 MAX POSITIVE DIFFERENCE = .255
- DIFFERENCE = .00003 MAX NEGATIVE DIFFERENCE = -.075

FIGURE 3.1.2

STAR Test 1 - IAEA 2D PWR Benchmark - 10 CM Mesh
IAEA 2D - 3 1/3 CM Mesh Nodal Reference

LEGEND

REFERENCE STAR % DIFFERENCE

	1	2	3	4	5	6	7	8	9
Y= 9									
Y= 8	.777	.757	.711						
	.781	.762	.717						
	.46	.71	.90						
Y= 7	.959	.976	1.000	.866	.611				
	.961	.977	1.002	.872	.619				
	.17	.07	.20	.75	1.24				
Y= 6	.953	1.055	1.089	.923	.700	.597			
	.953	1.053	1.088	.925	.706	.601			
	-.03	-.19	-.09	.23	.86	.67			
Y= 5	.610	1.072	1.181	.972	.476	.700	.611		
	.610	1.068	1.178	.971	.475	.706	.619		
	-.08	-.37	-.25	-.10	-.15	.86	1.24		
Y= 4	1.193	1.291	1.311	1.178	.972	.923	.866		
	1.186	1.283	1.307	1.174	.971	.925	.872		
	-.59	-.62	-.31	-.34	-.10	.23	.75		
Y= 3	1.422	1.432	1.368	1.311	1.181	1.089	1.000	.711	
	1.410	1.422	1.360	1.307	1.178	1.088	1.002	.717	
	-.84	-.70	-.58	-.31	-.25	-.09	.20	.90	
Y= 2	1.281	1.397	1.432	1.291	1.072	1.055	.976	.757	
	1.270	1.386	1.422	1.283	1.068	1.053	.977	.762	
	-.86	-.79	-.70	-.62	-.37	-.19	.07	.71	
Y= 1	.729	1.281	1.422	1.193	.610	.953	.959	.777	
	.727	1.270	1.410	1.186	.610	.953	.961	.781	
	-.22	-.86	-.84	-.59	-.08	-.03	.17	.46	

```
EIGENVALUE - REFERENCE  =  1.02903 STANDARD DEVIATION      =    .571
           - STAR       =  1.02911 MAX POSITIVE DIFFERENCE =   1.244
           - DIFFERENCE =   .00008 MAX NEGATIVE DIFFERENCE =   -.859
```

FIGURE 3.1.3

STAR Test 2 - IAEA 3D PWR Benchmark - ANL-7416(SUPP.2) P283
IAEA 3D - Venture Reference Solution

LEGEND

REFERENCE
STAR
% DIFFERENCE

	1	2	3	4	5	6	7	8	9
Y= 9									
Y= 8	.777	.757	.711						
	.780	.760	.715						
	.36	.39	.57						
Y= 7	.959	.976	1.000	.866	.611				
	.961	.977	1.001	.870	.615				
	.17	.09	.15	.41	.58				
Y= 6	.953	1.055	1.089	.923	.700	.597			
	.953	1.054	1.089	.924	.701	.601			
	-.04	-.05	-.02	.08	.18	.72			
Y= 5	.610	1.072	1.181	.972	.476	.700	.611		
	.610	1.069	1.178	.970	.477	.701	.615		
	-.02	-.29	-.21	-.20	.11	.18	.58		
Y= 4	1.193	1.291	1.311	1.178	.972	.923	.866		
	1.188	1.286	1.307	1.175	.970	.924	.870		
	-.38	-.39	-.32	-.23	-.20	.08	.41		
Y= 3	1.422	1.432	1.368	1.311	1.181	1.089	1.000	.711	
	1.416	1.425	1.363	1.307	1.178	1.089	1.001	.715	
	-.42	-.49	-.38	-.32	-.21	-.02	.15	.57	
Y= 2	1.281	1.397	1.432	1.291	1.072	1.055	.976	.757	
	1.274	1.390	1.425	1.286	1.069	1.054	.977	.760	
	-.51	-.47	-.49	-.39	-.29	-.05	.09	.39	
Y= 1	.729	1.281	1.422	1.193	.610	.953	.959	.777	
	.727	1.274	1.416	1.188	.610	.953	.961	.780	
	-.34	-.51	-.42	-.38	-.02	-.04	.17	.36	

EIGENVALUE - REFERENCE = 1.02903 STANDARD DEVIATION = .341
- STAR = 1.02909 MAX POSITIVE DIFFERENCE = .724
- DIFFERENCE = .00006 MAX NEGATIVE DIFFERENCE = -.507

FIGURE 3.1.4

STAR Test 2 - IAEA 3D PWR Benchmark - 10 CM Mesh - ANL-7416(SUPP.2) P
IAEA 3D - Venture Reference Solution

LEGEND

REFERENCE
STAR
% DIFFERENCE

Y= 11											
Y= 10											
Y= 9	.923	.867	.826	.853	.933	.974	.847				
Y= 8	1.480	1.281	1.171	1.220	1.423	1.680	1.623	1.328 1.329 .08			
Y= 7	1.662	1.149	.966	1.022	1.338	2.054	2.161 2.164 .14	1.621 1.623 .12	.846 .847 .01		
Y= 6	1.385	.939	.782	.843	1.151	1.852 1.853 .05	2.051 2.054 .15	1.679 1.680 .06	.972 .974 .21		
Y= 5	.789	.671	.618	.678	.864 .865 .13	1.152 1.151 -.09	1.339 1.338 -.07	1.422 1.423 .07	.933 .933 .04		
Y= 4	.511	.490	.492	.552 .552 .02	.678 .678 -.03	.843 .843 -.04	1.022 1.022	1.221 1.220 -.08	.853 .853		
Y= 3	.412	.4[illegible]6	.424 .424 -.05	.492 .492 -.02	.618 .618 -.05	.783 .782 -.05	.967 .966 -.09	1.173 1.171 -.17	.827 .826 -.05		
Y= 2	.440	.399 .399 -.03	.407 .406 -.12	.490 .490 -.10	.671 .671 .04	.940 .939 -.11	1.151 1.149 -.17	1.281 1.281	.867 .867 -.06		
Y= 1	.612 .612	.440 .440 -.16	.413 .412 -.12	.512 .511 -.14	.790 .789 -.20	1.386 1.385 -.07	1.661 1.662 .06	1.481 1.480 -.07	.924 .923 -.11		
	1	2	3	4	5	6	7	8	9	10	11

EIGENVALUE - REFERENCE = .99636 STANDARD DEVIATION = .094
- STAR = .99641 MAX POSITIVE DIFFERENCE = .206
- DIFFERENCE = .00005 MAX NEGATIVE DIFFERENCE = -.202

FIGURE 3.1.5

STAR Test 3 - LRA 2D Quarter Core Static Rods in Case
LRA 2D "Rods In" - Assembly Power Comparison

LEGEND

REFERENCE
STAR
% DIFFERENCE

	1	2	3	4	5	6	7
Y= 7							
Y= 6	.927	.842	.889	.914			
	.927	.842	.889	.914			
	-.01		-.01	-.04			
Y= 5	1.500	1.215	1.317	1.674	1.328		
	1.499	1.215	1.317	1.674	1.327		
	-.07				-.08		
Y= 4	1.522	.955	1.084	2.048	1.674	.914	
	1.522	.955	1.084	2.048	1.674	.914	
		.01				-.04	
Y= 3	.641	.568	.697	1.084	1.317	.889	
	.641	.568	.697	1.084	1.317	.889	
	.02	.02				-.01	
Y= 2	.423	.406	.568	.955	1.215	.842	
	.423	.406	.568	.955	1.215	.842	
	.02	.02	.02	.01			
Y= 1	.605	.423	.641	1.522	1.500	.927	
	.605	.423	.641	1.522	1.499	.927	
	.02	.02	.02		-.07	-.01	

EIGENVALUE - REFERENCE	= .99652	STANDARD DEVIATION	=	.026
- STAR	= .99652	MAX POSITIVE DIFFERENCE	=	.025
- DIFFERENCE	= -.00000	MAX NEGATIVE DIFFERENCE	=	-.075

FIGURE 3.1.6

<u>STAR Test 4 - LRA 3D Quarter Core Transient Extra Coarse Mesh 410 Time Steps</u>
<u>Assembly Power Comparison at Time = 0.0</u>

LEGEND

REFERENCE
STAR
% DIFFERENCE

	1	2	3	4	5	6	7
Y= 7							
Y= 6	.871	.799	.877	.940			
	.857	.791	.876	.946			
	-1.54	-1.03	-.14	.69			
Y= 5	1.407	1.153	1.304	1.738	1.461		
	1.385	1.140	1.303	1.753	1.478		
	-1.56	-1.13	-.08	.86	1.16		
Y= 4	1.424	.906	1.079	2.140	1.917	1.086	
	1.403	.896	1.079	2.169	1.972	1.127	
	-1.47	-1.10		1.36	2.87	3.78	
Y= 3	.601	.538	.687	1.111	1.390	.947	
	.591	.532	.685	1.116	1.396	.952	
	-1.55	-1.13	-.22	.45	.43	.58	
Y= 2	.396	.383	.545	.928	1.189	.826	
	.389	.377	.540	.921	1.182	.822	
	-1.72	-1.41	-.95	-.71	-.59	-.51	
Y= 1	.564	.397	.610	1.455	1.442	.893	
	.553	.391	.602	1.439	1.425	.883	
	-1.88	-1.61	-1.29	-1.10	-1.18	-1.13	

STANDARD DEVIATION = 1.318
MAX POSITIVE DIFFERENCE = 3.775
MAX NEGATIVE DIFFERENCE = -1.881

FIGURE 3.1.7

STAR Test 4 - LRA 3D Quarter Core Transient Extra Coarse Mesh 410 Time Steps
Assembly Power Comparison at Time = 0.4 Sec

LEGEND

REFERENCE
STAR
% DIFFERENCE

	1	2	3	4	5	6	7
Y= 7							
Y= 6	.513	.542	.820	1.107			
	.515	.544	.820	1.106			
	.47	.31	.02	-.09			
Y= 5	.826	.782	1.248	2.145	2.175		
	.830	.785	1.249	2.142	2.169		
	.47	.32	.08	-.14	-.28		
Y= 4	.835	.614	1.067	2.769	3.280	2.067	
	.839	.620	1.067	2.766	3.272	2.060	
	.49	1.04		-.11	-.24	-.34	
Y= 3	.354	.366	.639	1.288	1.789	1.262	
	.356	.367	.639	1.286	1.785	1.259	
	.45	.30	.05	-.16	-.22	-.24	
Y= 2	.223	.241	.414	.768	1.024	.723	
	.224	.242	.414	.769	1.025	.724	
	.49	.37	.19	.13	.10	.10	
Y= 1	.303	.235	.416	1.040	1.054	.661	
	.305	.236	.418	1.043	1.057	.663	
	.53	.43	.31	.29	.28	.24	

STANDARD DEVIATION = .304
MAX POSITIVE DIFFERENCE = 1.043
MAX NEGATIVE DIFFERENCE = -.339

FIGURE 3.1.8

STAR Test 4 - LRA 3D Quarter Core Transient Extra Coarse Mesh 410 Time Steps
Assembly Power Comparison at Time = 0.8 Sec

LEGEND

REFERENCE
STAR
% DIFFERENCE

	1	2	3	4	5	6	7
Y= 7							
Y= 6	.573	.580	.810	1.059			
	.566	.576	.809	1.061			
	-1.13	-.71	-.10	.19			
Y= 5	.921	.834	1.222	2.032	2.083		
	.911	.828	1.222	2.039	2.089		
	-1.12	-.71		.34	.29		
Y= 4	.932	.659	1.039	2.615	3.148	2.011	
	.923	.655	1.041	2.633	3.178	2.030	
	-.96	-.65	.19	.69	.95	.94	
Y= 3	.400	.396	.637	1.244	1.736	1.236	
	.396	.393	.637	1.247	1.738	1.237	
	-1.15	-.78	-.09	.24	.12	.08	
Y= 2	.263	.273	.439	.795	1.056	.747	
	.259	.270	.436	.791	1.051	.744	
	-1.48	-1.21	-.68	-.49	-.47	-.40	
Y= 1	.369	.274	.457	1.116	1.127	.708	
	.363	.270	.452	1.108	1.118	.702	
	-1.73	-1.42	-.99	-.72	-.80	-.83	

STANDARD DEVIATION = .698
MAX POSITIVE DIFFERENCE = .953
MAX NEGATIVE DIFFERENCE = -1.733

FIGURE 3.1.9

STAR Test 4 - LRA 3D Quarter Core Transient Extra Coarse Mesh 410 Time Steps
Assembly Power Comparison at Time = 1.0 Sec

LEGEND

REFERENCE
STAR
% DIFFERENCE

Y= 7							
Y= 6	.460	.491	.765	1.091			
	.466	.496	.768	1.087			
	1.24	1.12	.42	-.37			
Y= 5	.738	.705	1.162	2.130	2.369		
	.748	.713	1.167	2.122	2.343		
	1.30	1.12	.43	-.38	-1.10		
Y= 4	.748	.560	1.003	2.798	3.761	2.488	
	.759	.566	1.006	2.791	3.740	2.469	
	1.39	1.00	.30	-.25	-.56	-.76	
Y= 3	.324	.338	.606	1.286	1.883	1.365	
	.328	.341	.608	1.282	1.868	1.353	
	1.39	1.04	.35	-.31	-.80	-.88	
Y= 2	.213	.229	.390	.728	.985	.704	
	.216	.231	.392	.730	.987	.706	
	1.36	1.09	.64	.32	.22	.18	
Y= 1	.296	.225	.389	.963	.981	.622	
	.301	.228	.392	.970	.987	.625	
	1.48	1.24	.93	.74	.58	.48	
	1	2	3	4	5	6	7

STANDARD DEVIATION = .766
MAX POSITIVE DIFFERENCE = 1.484
MAX NEGATIVE DIFFERENCE = -1.098

FIGURE 3.1.10

STAR Test 4 - LRA 3D Quarter Core Transient Extra Coarse Mesh 410 Time Steps
Assembly Power Comparison at Time = 2.0 Sec

LEGEND

REFERENCE
STAR
% DIFFERENCE

		1	2	3	4	5	6	7
Y= 7								
Y= 6	REFERENCE	.494	.515	.769	1.072			
	STAR	.495	.518	.772	1.071			
	% DIFFERENCE	.36	.47	.33	-)9			
Y= 5	REFERENCE	.792	.740	1.164	2.082	2.290		
	STAR	.795	.743	1.168	2.082	2.279		
	% DIFFERENCE	.39	.46	.34		-.4(		
Y= 4	REFERENCE	.804	.587	1.000	2.733	3.639	2.405	
	STAR	.808	.590	1.003	2.732	3.616	2.384	
	% DIFFERENCE	.47	.43	.30	-.04	-.63	-.87	
Y= 3	REFERENCE	.350	.356	.610	1.266	1.840	1.333	
	STAR	.351	.358	.613	1.267	1.836	1.329	
	% DIFFERENCE	.43	.45	.38	.08	-.22	-.30	
Y= 2	REFERENCE	.234	.246	.405	.744	1.000	.714	
	STAR	.235	.247	.406	.746	1.002	.715	
	% DIFFERENCE	.34	.37	.37	.24	.20	.18	
Y= 1	REFERENCE	.329	.245	.410	1.005	1.019	.644	
	STAR	.330	.246	.412	1.008	1.021	.645	
	% DIFFERENCE	.30	.33	.34	.30	.20	.19	

STANDARD DEVIATION = .333
MAX POSITIVE DIFFERENCE = .472
MAX NEGATIVE DIFFERENCE = -.873

FIGURE 3.1.11

STAR Test 4 - LRA 3D Quarter Core Transient Extra Coarse Mesh 410 Time Steps
Assembly Power Comparison at Time = 3.0 Sec

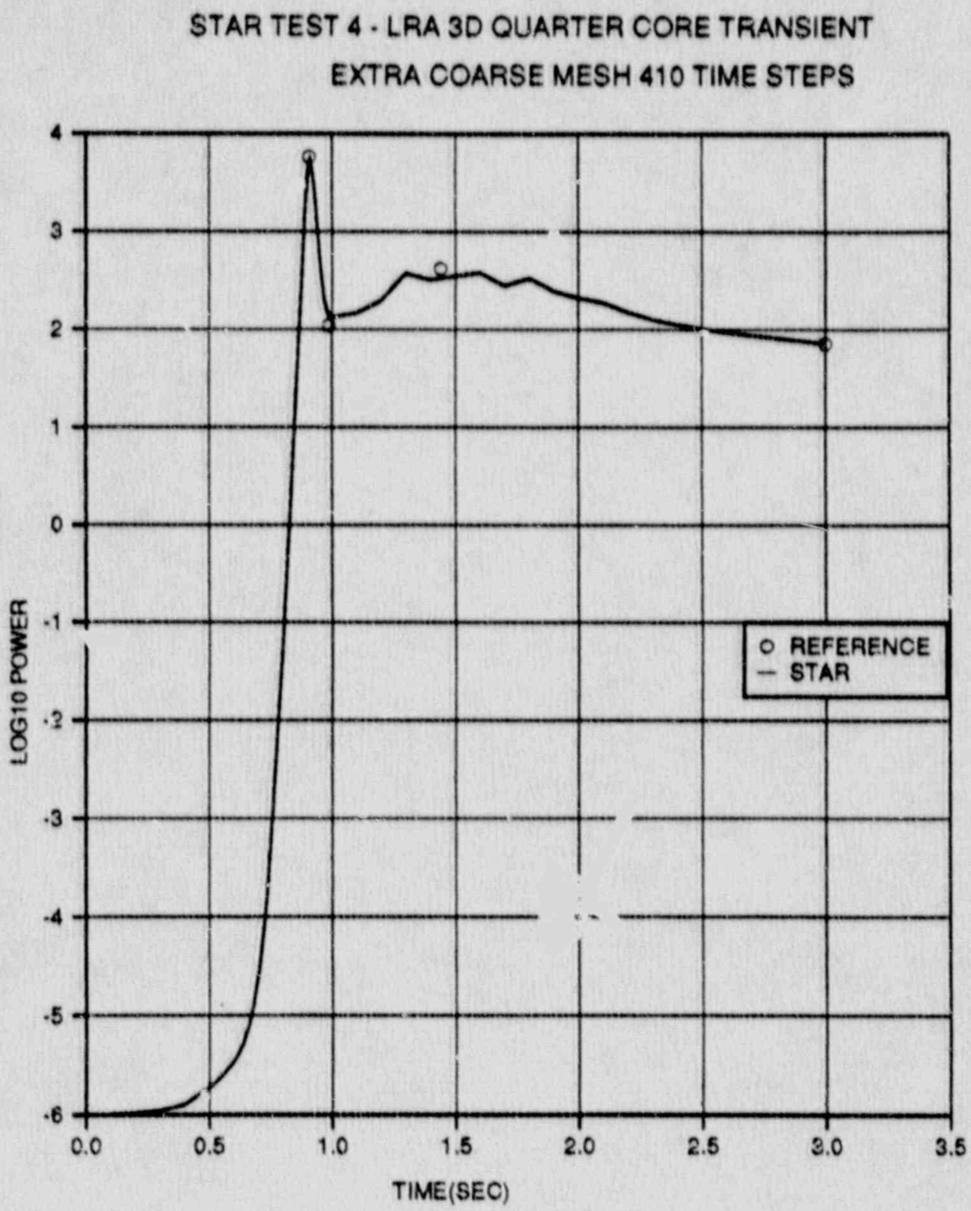

FIGURE 3.1.12

STAR Test 4 - LRA 3D Quarter Core Transient
Extra Coarse Mesh 410 Time Steps

LEGEND

REFERENCE
STAR
% DIFFERENCE

Y= 11											
Y= 10											
Y= 9	.923	.867	.826	.853	.933	.973	.846				
	.923	.867	.826	.853	.933	.973	.846				
	-.01	-.01			.01		.01				
Y= 8	1.481	1.281	1.171	1.220	1.423	1.680	1.623	1.329			
	1.481	1.281	1.171	1.220	1.423	1.680	1.623	1.329			
Y= 7	1.663	1.149	.966	1.022	1.338	2.053	2.164	1.623	.846		
	1.662	1.149	.966	1.022	1.338	2.054	2.164	1.623	.846		
	-.06					.05			.01		
Y= 6	1.386	.939	.782	.843	1.151	1.853	2.053	1.680	.973		
	1.386	.939	.782	.843	1.151	1.853	2.054	1.680	.973		
							.05				
Y= 5	.789	.671	.618	.678	.865	1.151	1.338	1.423	.933		
	.789	.671	.618	.678	.865	1.151	1.338	1.423	.933		
	-.01	-.01							.01		
Y= 4	.511	.490	.492	.553	.678	.843	1.022	1.220	.853		
	.511	.490	.492	.552	.678	.843	1.022	1.220	.853		
			-.02	-.02							
Y= 3	.413	.406	.424	.492	.618	.782	.966	1.171	.826		
	.413	.406	.424	.492	.618	.782	.966	1.171	.826		
	-.02	-.02		-.02							
Y= 2	.440	.400	.406	.490	.671	.939	1.149	1.281	.867		
	.440	.400	.406	.490	.671	.939	1.149	1.281	.867		
	-.02		-.02		-.01				-.01		
Y= 1	.613	.440	.413	.511	.789	1.386	1.663	1.481	.923		
	.613	.440	.413	.511	.789	1.386	1.662	1.481	.923		
	-.02	-.02	-.02		-.01		-.06		-.01		
	1	2	3	4	5	6	7	8	9	10	11

EIGENVALUE - REFERENCE = .99636 STANDARD DEVIATION = .015
- STAR = .99641 MAX POSITIVE DIFFERENCE = .049
- DIFFERENCE = .00005 MAX NEGATIVE DIFFERENCE = -.060

FIGURE 3.1.13

STAR Test 9 - LRA 2D Quarter Core Transient Coarse Mesh 329 Time Steps
Assembly Power Comparison at Time = 0.0 Sec

LEGEND

REFERENCE
STAR
% DIFFERENCE

	1	2	3	4	5	6	7	8	9	10	11
Y= 11											
Y= 10											
Y= 9	.846	.802	.782	.832	.938	1.006	.896				
	.847	.803	.782	.832	.937	1.005	.895				
	.12	.10	.03		-.09	-.10	-.11				
Y= 8	1.355	1.185	1.109	1.193	1.439	1.749	1.741	1.480			
	1.357	1.186	1.109	1.193	1.438	1.747	1.740	1.479			
	.15	.08			-.07	-.11	-.06	-.07			
Y= 7	1.520	1.062	.915	1.002	1.361	2.153	2.352	1.890	1.024		
	1.522	1.063	.915	1.002	1.360	2.151	2.349	1.892	1.025		
	.13	.09	.02		-.07	-.09	-.13	.11	.10		
Y= 6	1.267	.867	[illegible]	.828	1.172	1.943	2.231	1.949	1.163		
	1.268	.868	.741	.827	1.171	1.941	2.229	1.951	1.164		
	.08	.09	.05	-.05	-.09	-.10	-.09	.10	.09		
Y= 5	.721	.620	.584	.662	.873	1.193	1.424	1.554	1.032		
	.722	.620	.584	.662	.872	1.192	1.423	1.553	1.031		
	.11	.10	.02	-.02	-.09	-.08	-.07	-.06	-.10		
Y= 4	.467	.452	.463	.534	.671	.851	1.048	1.264	.889		
	.468	.452	.463	.533	.670	.850	1.047	1.263	.888		
	.13	.07	.04	-.04	-.04	-.08	-.10	-.08	-.01		
Y= 3	.376	.373	.396	.468	.596	.764	.951	1.161	.822		
	.376	.373	.396	.468	.596	.764	.951	1.161	.821		
	.08	.08	.03	.02	-.03	-.01	-.04		-.02		
Y= 2	.398	.365	.376	.460	.635	.894	1.099	1.231	.835		
	.399	.365	.376	.460	.636	.894	1.100	1.231	.836		
	.13	.08	.08		.03	-.01	.09		.04		
Y= 1	.553	.399	.380	.476	.741	1.306	1.571	[illegible]	.877		
	.554	.400	.380	.477	.741	1.307	1.572	1.405	.878		
	.14	.13	.08	.06	.03	.08	.06	.07	.02		

STANDARD DEVIATION = .077
MAX POSITIVE DIFFERENCE = .148
MAX NEGATIVE DIFFERENCE = -.128

FIGURE 3.1.14

STAR Test 9 - LRA 2D Quarter Core Transient Coarse Mesh 329 Time Steps
Assembly Power Comparison at Time = 0.4 Sec

LEGEND

REFERENCE
STAR
% DIFFERENCE

Y	1	2	3	4	5	6	7	8	9	10	11
Y= 11											
Y= 10											
Y= 9	.736	.711	.719	.802	.946	1.051	.966				
	.737	.712	.719	.802	.944	1.050	.965				
	.19	.17	.03	-.01	-.14	-.10	-.17				
Y= 8	1.177	1.048	1.020	1.155	1.461	1.846	1.910	1.695			
	1.180	1.049	1.021	1.154	1.460	1.843	1.908	1.693			
	.25	.10	.10	-.09	-.07	-.16	-.10	-.12			
Y= 7	1.317	.937	.842	.975	1.394	2.293	2.617	2.272	1.283		
	1.320	.939	.842	.975	1.392	2.290	2.613	2.274	1.284		
	.23	.18	.01	-.02	-.14	-.13	-.15	.09	.08		
Y= 6	1.097	.764	.682	.806	1.202	2.070	2.481	2.332	1.436		
	1.100	.765	.683	.805	1.201	2.067	2.479	2.333	1.438		
	.27	.13	.07	-.07	-.08	-.14	-.08	.04	.14		
Y= 5	.625	.547	.537	.640	.883	1.253	1.546	1.738	1.173		
	.626	.548	.537	.640	.882	1.252	1.544	1.737	1.172		
	.18	.16	.02	-.03	-.14	-.08	-.13	-.06	-.09		
Y= 4	.405	.398	.422	.506	.660	.861	1.084	1.326	.939		
	.405	.399	.422	.506	.660	.860	1.084	1.325	.939		
	.20	.10	.07	-.06	-.06	-.13		-.08	-.02		
Y= 3	.323	.326	.355	.433	.566	.738	.931	1.146	.815		
	.324	.326	.355	.433	.566	.738	.931	1.146	.815		
	.19	.18	.03	.02	-.05		-.04		-.01		
Y= 2	.339	.315	.332	.416	.585	.830	1.029	1.160	.791		
	.340	.315	.333	.416	.585	.830	1.030	1.160	.791		
	.27	.16	.12	.05	.09	.04	.10		.09		
Y= 1	.468	.342	.333	.427	.672	1.193	1.442	1.295	.812		
	.469	.343	.333	.427	.673	1.194	1.443	1.297	.813		
	.28	.23	.12	.12	.07	.08	.07	.15	.10		

STANDARD DEVIATION	=	.121
MAX POSITIVE DIFFERENCE	=	.278
MAX NEGATIVE DIFFERENCE	=	-.166

FIGURE 3.1.15

STAR Test 9 - LRA 2D Quarter Core Transient Coarse Mesh 329 Time Steps
Assembly Power Comparison at Time = 0.8 Sec

LEGEND

REFERENCE
STAR
% DIFFERENCE

Y= 11											
Y= 10											
Y= 9	.597	.595	.637	.760	.946	1.101	1.050				
	.597	.594	.636	.760	.948	1.102	1.050				
	-.08	-.03	-.09	-.01	-.04	.09					
Y= 8	.953	.875	.905	1.100	1.479	1.958	2.119	1.972			
	.953	.874	.904	1.099	1.480	1.958	2.121	1.973			
	-.03	-.11	-.03	-.09	.07		.09	.05			
Y= 7	1.064	.780	.749	.936	1.427	2.458	2.952	2.784	1.641		
	1.063	.779	.748	.936	1.427	2.460	2.953	2.789	1.642		
	-.09	-.05	-.12	-.02		.08	.03	.18	.06		
Y= 6	.885	.636	.607	.776	1.233	2.223	2.799	2.848	1.812		
	.885	.635	.607	.775	1.233	2.223	2.802	2.850	1.816		
	-.05	-.14	-.07	-.10			.11	.07	.22		
Y= 5	.506	.456	.476	.610	.893	1.324	1.701	1.979	1.361		
	.505	.456	.475	.610	.893	1.325	1.701	1.981	1.361		
	-.12	-.09	-.15	-.05	-.08	.08		.10			
Y= 4	.327	.331	.370	.471	.645	.873	1.129	1.404	1.003		
	.327	.331	.369	.470	.644	.872	1.129	1.404	1.004		
	-.12	-.18	-.11	-.15	-.05	-.08			.10		
Y= 3	.259	.268	.305	.389	.526	.702	.902	1.123	.803		
	.258	.267	.304	.388	.525	.702	.902	1.123	.803		
	-.19	-.11	-.20	-.10	-.15	-.04	-.08		-.05		
Y= 2	.267	.253	.278	.361	.519	.746	.935	1.065	.730		
	.267	.253	.278	.361	.519	.745	.935	1.065	.731		
	-.11	-.20	-.14	-.17	-.08	-.09	-.01		.01		
Y= 1	.364	.272	.275	.364	.584	1.044	1.272	1.151	.725		
	.363	.271	.274	.364	.584	1.044	1.271	1.151	.725		
	-.11	-.11	-.18	-.08	-.09		-.08		-.04		
	1	2	3	4	5	6	7	8	9	10	11

STANDARD DEVIATION = .087
MAX POSITIVE DIFFERENCE = .221
MAX NEGATIVE DIFFERENCE = -.197

FIGURE 3.1.16

STAR Test 9 - LRA 2D Quarter Core Transient Coarse Mesh 329 Time Steps
Assembly Power Comparison at Time = 1.2 Sec

LEGEND

REFERENCE STAR % DIFFERENCE

	1	2	3	4	5	6	7	8	9	10	11
Y= 11											
Y= 10											
Y= 9	.541	.546	.600	.735	.940	1.112	1.077				
	.539	.544	.599	.735	.940	1.113	1.079				
	-.39	-.31	-.22	-.07	.02	.09	.19				
Y= 8	.863	.804	.854	1.069	1.473	1.989	2.197	2.092			
	.860	.801	.852	1.068	1.474	1.992	2.201	2.096			
	-.38	-.32	-.19	-.09	.07	.15	.18	.19			
Y= 7	.962	.716	.708	.913	1.429	2.509	3.088	3.036	1.826		
	.958	.714	.707	.913	1.431	2.513	3.094	3.044	1.830		
	-.39	-.32	-.20	-.02	.14	.16	.19	.26	.22		
Y= 6	.801	.584	.575	.759	1.237	2.273	2.932	3.104	2.008		
	.798	.582	.574	.759	1.238	2.276	2.938	3.111	2.013		
	-.40	-.34	-.19	-.04	.08	.13	.20	.23	.25		
Y= 5	.459	.420	.451	.595	.892	1.348	1.765	2.089	1.449		
	.457	.419	.450	.595	.893	1.349	1.767	2.093	1.451		
	-.41	-.33	-.22	-.05	.04	.07	.11	.19	.14		
Y= 4	.297	.305	.349	.455	.636	.874	1.145	1.435	1.030		
	.296	.304	.348	.454	.635	.874	1.146	1.436	1.030		
	-.44	-.39	-.26	-.13	-.03	.02	.09	.07			
Y= 3	.235	.245	.285	.370	.508	.685	.887	1.109	.796		
	.234	.244	.284	.369	.507	.684	.887	1.109	.795		
	-.51	-.45	-.35	-.22	-.16	-.09	-.07		-.06		
Y= 2	.240	.231	.257	.339	.491	.709	.892	1.021	.701		
	.239	.229	.256	.338	.490	.707	.891	1.019	.700		
	-.58	-.52	-.39	-.32	-.24	-.23	-.18	-.20	-.16		
Y= 1	.326	.246	.252	.338	.546	.978	1.195	1.085	.685		
	.324	.245	.251	.337	.545	.976	1.192	1.082	.683		
	-.58	-.53	-.48	-.35	-.29	-.26	-.25	-.28	-.25		

STANDARD DEVIATION = .233
MAX POSITIVE DIFFERENCE = .264
MAX NEGATIVE DIFFERENCE = -.583

FIGURE 3.1.17

STAR Test 9 - LRA 2D Quarter Core Transient Coarse Mesh 329 Time Steps
Assembly Power Comparison at Time = 1.4 Sec

LEGEND

REFERENCE STAR % DIFFERENCE

	1	2	3	4	5	6	7	8	9	10	11
Y= 11											
Y= 10											
Y= 9	.463	.473	.532	.671	.882	1.079	1.093				
	.460	.471	.531	.670	.883	1.080	1.095				
	-.58	-.51	-.23	-.12	.09	.09	.18				
Y= 8	.735	.693	.754	.972	1.383	1.942	2.271	2.335			
	.730	.690	.752	.972	1.383	1.945	2.273	2.341			
	-.68	-.45	-.32	-.03		.15	.09	.26			
Y= 7	.820	.617	.626	.834	1.352	2.480	3.271	3.648	2.356		
	.815	.613	.625	.833	1.354	2.481	3.277	3.656	2.365		
	-.62	-.55	-.21	-.07	.15	.04	.18	.22	.38		
Y= 6	.686	.506	.512	.698	1.179	2.259	3.118	3.723	2.552		
	.682	.504	.511	.698	1.179	2.263	3.121	3.734	2.559		
	-.70	-.45	-.27	.04		.18	.10	.30	.27		
Y= 5	.397	.368	.405	.550	.850	1.330	1.833	2.294	1.654		
	.395	.366	.404	.549	.851	1.331	1.836	2.298	1.658		
	-.58	-.52	-.17	-.07	.12	.08	.16	.17	.24		
Y= 4	.262	.272	.316	.421	.600	.846	1.142	1.472	1.080		
	.260	.271	.315	.420	.600	.847	1.142	1.474	1.081		
	-.65	-.41	-.28	-.05	-.05	.11		.14	.09		
Y= 3	.211	.221	.259	.340	.470	.642	.845	1.073	.781		
	.209	.220	.258	.339	.470	.641	.845	1.072	.782		
	-.57	-.54	-.31	-.26	-.06	-.14	-.01	-.09	.05		
Y= 2	.219	.210	.234	.308	.445	.643	.814	.941	.654		
	.217	.209	.233	.307	.444	.641	.811	.939	.653		
	-.78	-.57	-.51	-.29	-.34	-.23	-.31	-.18	-.23		
Y= 1	.299	.225	.229	.305	.489	.874	1.069	.975	.622		
	.297	.223	.228	.304	.488	.870	1.065	.971	.620		
	-.80	-.76	-.52	-.49	-.35	-.45	-.37	-.40	-.29		

STANDARD DEVIATION = .305
MAX POSITIVE DIFFERENCE = .382
MAX NEGATIVE DIFFERENCE = -.802

FIGURE 3.1.18

STAR Test 9 - LRA 2D Quarter Core Transient Coarse Mesh 329 Time Steps
Assembly Power Comparison at Time = 2.0 Sec

LEGEND

REFERENCE
STAR
% DIFFERENCE

Y	1	2	3	4	5	6	7	8	9	10	11
Y= 11											
Y= 10											
Y= 9	.505	.508	.556	.681	.876	1.058	1.062				
	.499	.504	.553	.680	.877	1.060	1.066				
	-.99	-.85	-.49	-.18	.14	.19	.38				
Y= 8	.802	.744	.787	.984	1.368	1.893	2.196	2.248			
	.793	.738	.783	.983	1.370	1.900	2.205	2.259			
	-1.06	-.82	-.53	-.10	.15	.37	.41	.49			
Y= 7	.896	.664	.653	.842	1.332	2.411	3.154	3.503	2.261		
	.887	.658	.650	.841	1.335	2.419	3.168	3.520	2.[illegible]1		
	-1.04	-.90	-.47	-.12	.23	.33	.44	.49	.57		
Y= 6	.752	.546	.535	.704	1.162	2.197	3.010	3.577	2.453		
	.743	.541	.532	.704	1.164	2.205	3.022	3.595	2.465		
	-1.09	-.88	-.54	-.07	.17	.36	.40	.50	.49		
Y= 5	.436	.398	.425	.559	.843	1.302	1.778	2.220	1.600		
	.431	.395	.423	.558	.845	1.305	1.785	2.228	1.607		
	-1.06	-.93	-.52	-.20	.14	.23	.39	.36	.44		
Y= 4	.289	.296	.335	.434	.605	.841	1.126	1.446	1.062		
	.286	.293	.333	.432	.605	.841	1.127	1.450	1.064		
	-1.14	-.98	-.69	-.30	-.10	.11	.09	.28	.19		
Y= 3	.236	.244	.279	.357	.485	.654	.853	1.081	.786		
	.233	.242	.277	.355	.483	.652	.852	1.079	.786		
	-1.27	-1.15	-.82	-.59	-.33	-.24	-.11	-.19	-.04		
Y= 2	.249	.235	.256	.329	.469	.671	.844	.971	.674		
	.245	.232	.253	.327	.466	.667	.840	.967	.672		
	-1.49	-1.23	-1.05	-.76	-.64	-.49	-.49	-.38	-.40		
Y= 1	.343	.254	.253	.329	.520	.923	1.122	1.020	.650		
	.338	.250	.250	.326	.517	.917	1.115	1.014	.646		
	-1.52	-1.42	-1.11	-.88	-.71	-.69	-.62	-.59	-.52		

STANDARD DEVIATION = .583
MAX POSITIVE DIFFERENCE = .575
MAX NEGATIVE DIFFERENCE = -1.517

FIGURE 3.1.19

STAR Test 9 - LRA 2D Quarter Core Transient Coarse Mesh 329 Time Steps
Assembly Power Comparison at Time = 3.0 Sec

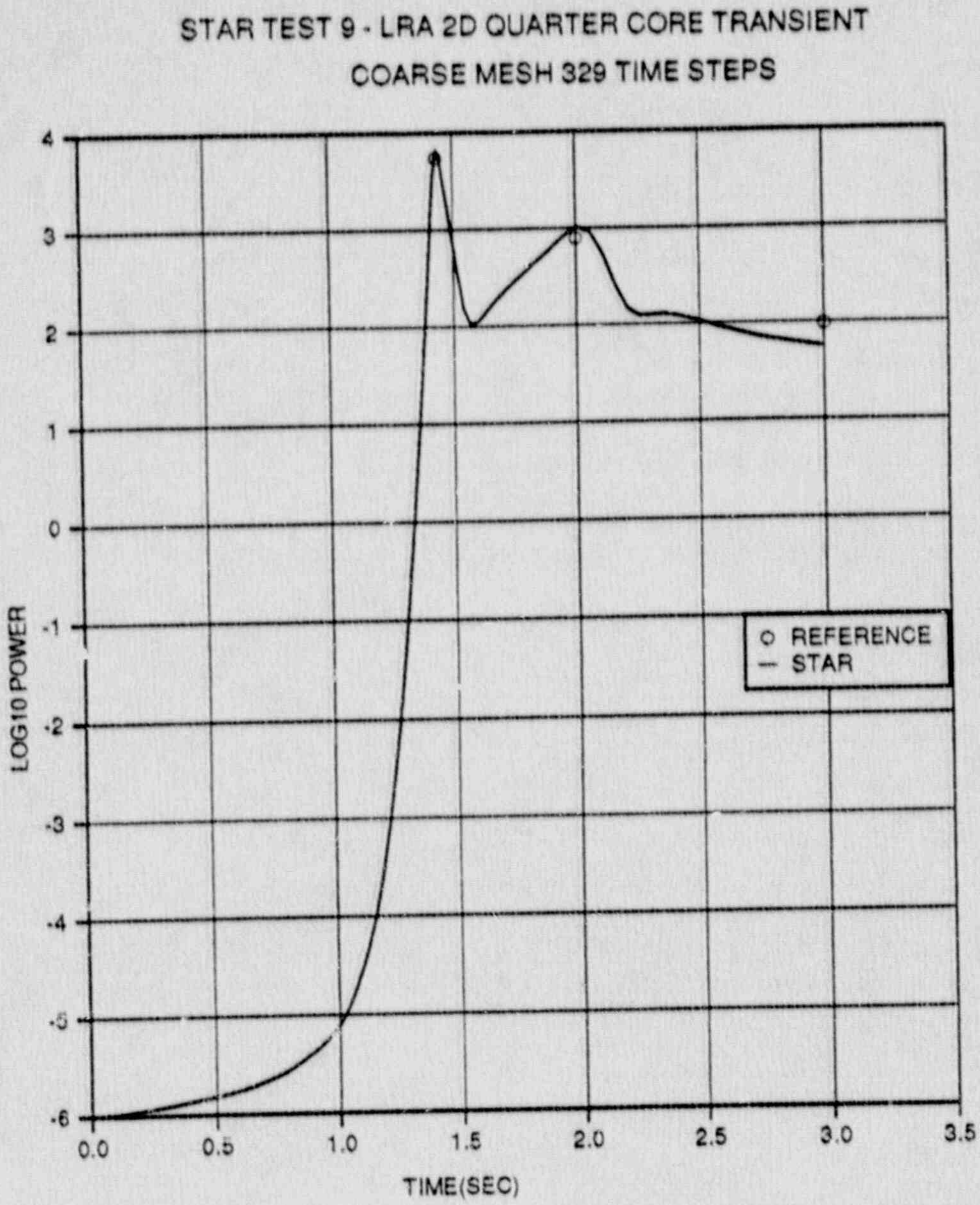

FIGURE 3.1.20

STAR Test 9 - LRA 2D Quarter Core Transient
Coarse Mesh 329 Time Steps

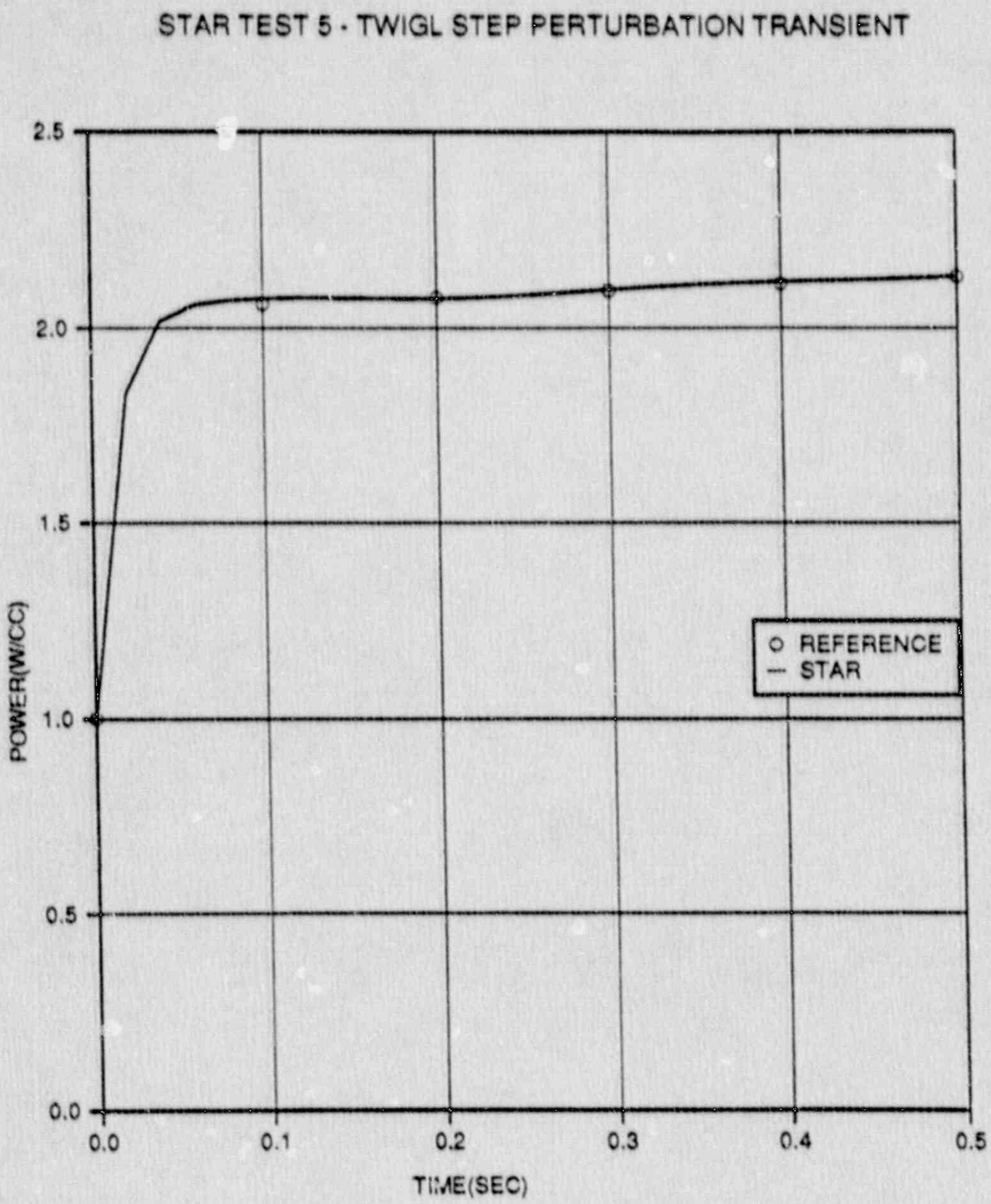

FIGURE 3.1.21

STAR Test 5 - TWIGL Step Perturbation Transient

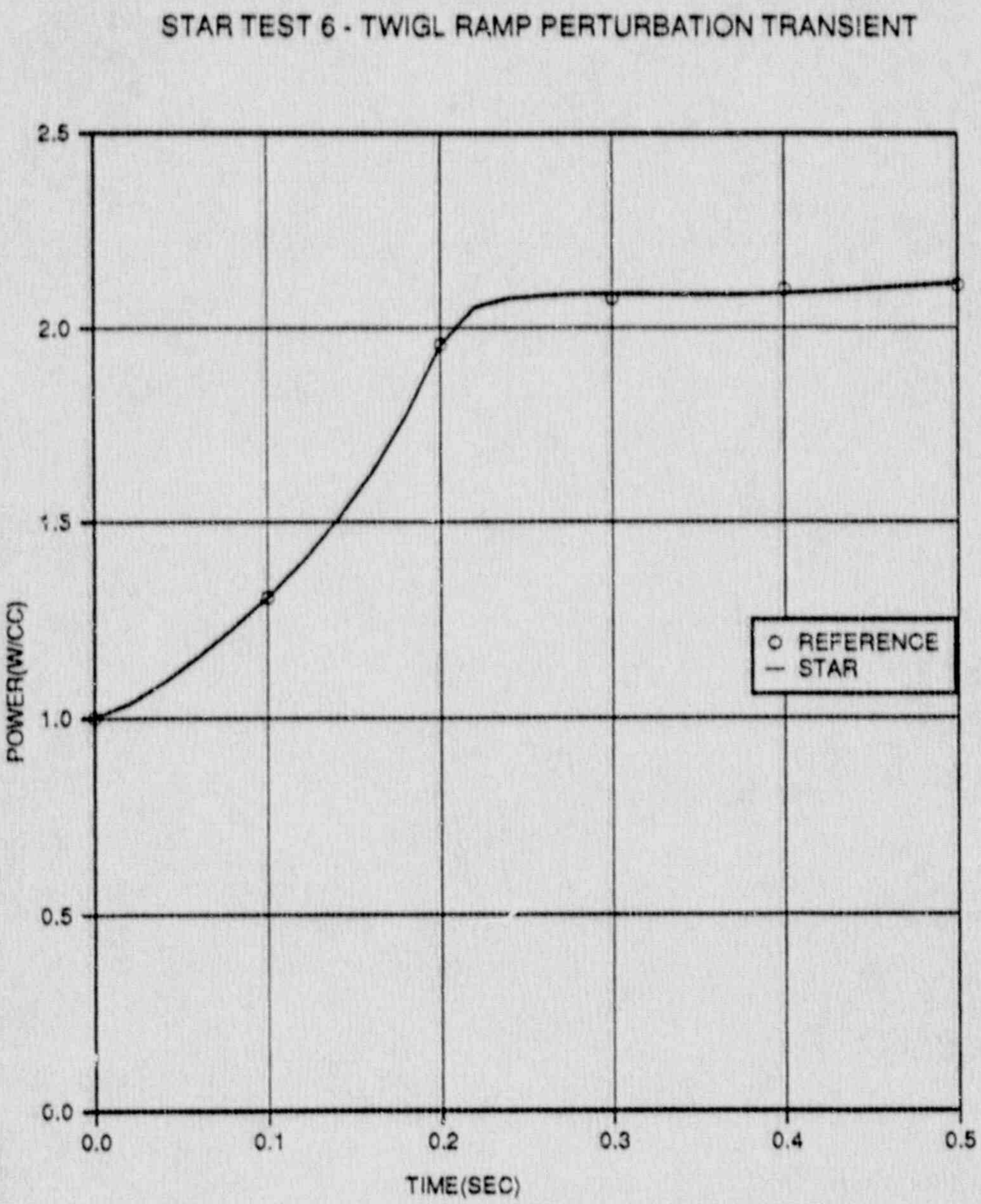

FIGURE 3.1.22

STAR Test 6 - TWIGL Ramp Perturbation Transient

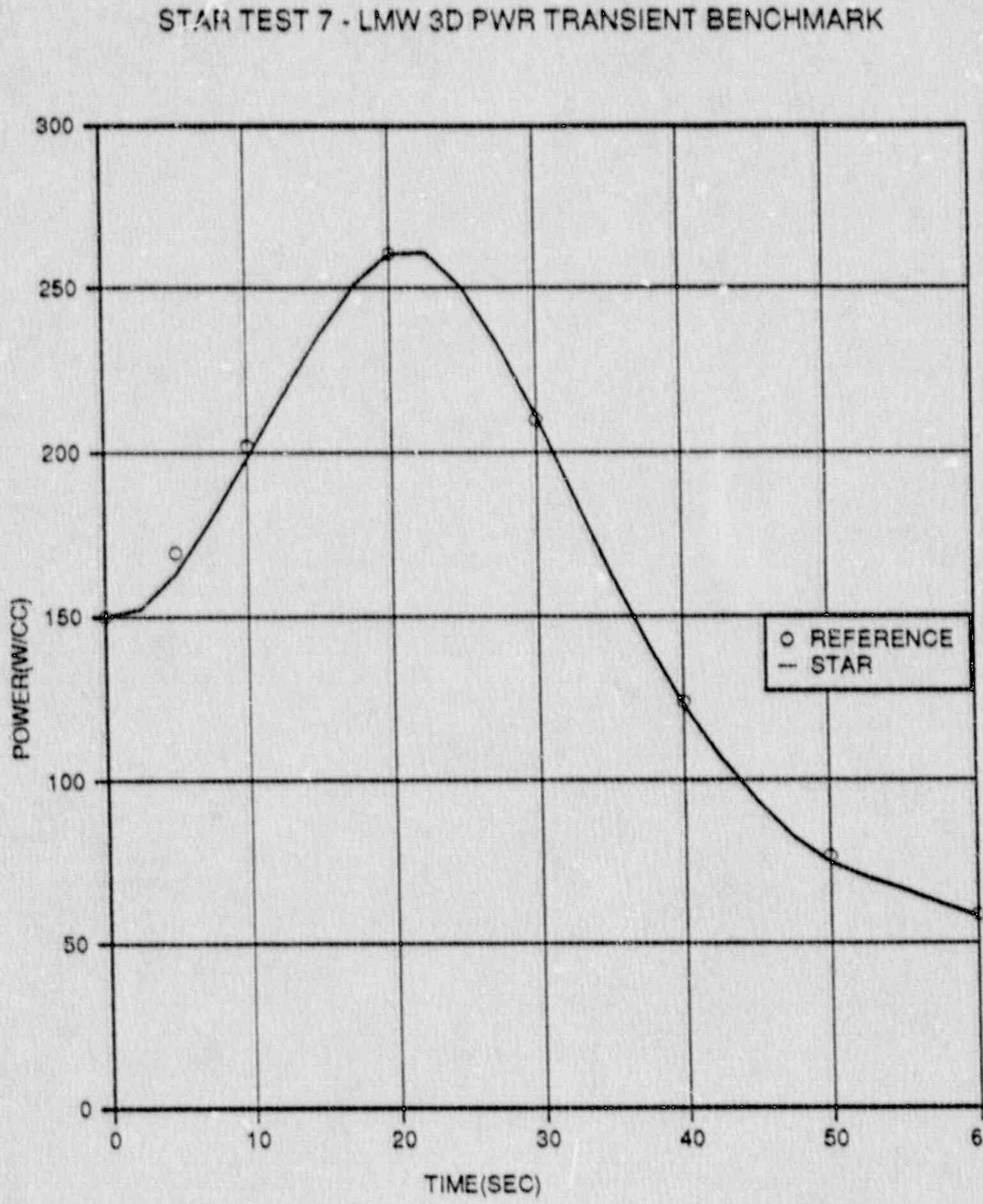

FIGURE 3.1.23

STAR Test 7 - LMW 3D PWR Transient Benchmark

LEGEND

REFERENCE
STAR
% DIFFERENCE

Y= 6						
Y= 5						
	.727	.708	.630	.434		
Y= 4				.860	.434	
	.980	1.083	.982	.864	.434	
				.47	-.14	
Y= 3			1.123	.980	.627	
	1.438	1.394	1.122	.982	.630	
			-.07	.15	.35	
Y= 2		1.589	1.396	1.083	.708	
	1.652	1.587	1.394	1.083	.708	
		-.15	-.14	-.03		
Y= 1	1.554	1.654	1.440	.980	.727	
	1.551	1.652	1.438	.980	.727	
	-.21	-.15	-.15	-.03	-.01	
	1	2	3	4	5	6

EIGENVALUE - REFERENCE =	.99974	STANDARD DEVIATION	=	.199
- STAR =	.99973	MAX POSITIVE DIFFERENCE	=	.465
- DIFFERENCE =	-.00001	MAX NEGATIVE DIFFERENCE	=	-.206

FIGURE 3.1.24

STAR Test 7 - LMW 3D PWR Transient Benchmark
Assembly Power Comparison at Time = 0.0 Sec

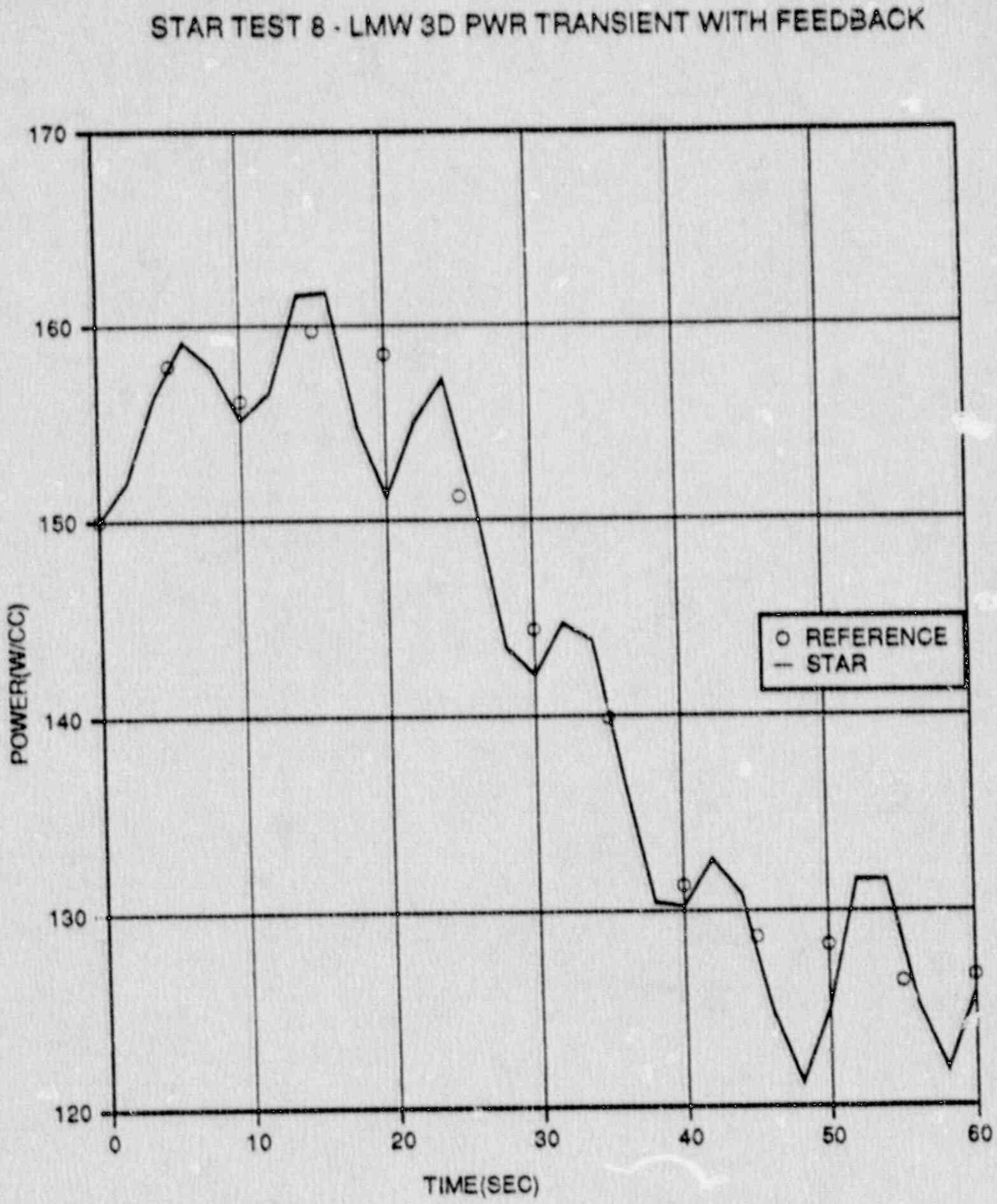

FIGURE 3.1.25

STAR Test 8 - LMW 3D PWR Transient with Feedback

3.2 EPRI HERMITE Comparison

3.2.1 Introduction

As part of the verification for the ARROTTA[26] computer code, the Electric Power Research Institute commissioned a comparison of the results from ARROTTA to the results from Combustion Engineering's HERMITE code[27]. The HERMITE code has been approved by the NRC and has been applied in a variety of licensing analyses.

The ARROTTA input deck[28] was converted to a STAR input deck with options chosen to make the problems as similar as possible. The layout is shown in Figure 3.2.1. The ARROTTA cross sections were converted to a SIMULATE-3 run time library containing cross sections for all the ARROTTA comparisons with no assembly discontinuity factors. The VIPRE-01 code was chosen as a thermal hydraulic feedback model with no gap connections between channels and default material properties in the fuel rod model.

STAR was run with one neutronic mesh and one thermal hydraulic mesh per assembly as in the ARROTTA case reported. STAR uses the same mesh for neutronic and hydraulic calculations.

3.2.2 Static Results

The same series of steady-state cases were run for STAR as for HERMITE (and ARROTTA) and the three-dimensional transients were run for several different time steps.

The first static case is the all rods out, hot zero power case which demonstrates consistent modelling without control rod and thermal-hydraulic feedback effects. Agreement for this case is good as shown by Figure 3.2.2.

Next an all rods out hot full power case was run to demonstrate the effect of thermal-hydraulic feedback on the cross sections. Figure 3.2.3 shows the excellent agreement achieved in radial power distribution and eigenvalue. The highest planar average fuel temperature from STAR was about 1375 °F, about 85 °F lower than the HERMITE peak value of 1460 °F.

A rodded case at hot zero power was run to represent the initial conditions for the transient. Figure 3.2.4 shows good agreement for this case also.

Finally a hot zero power case with the ejected rod out was run. The radial power and eigenvalue are shown in Figure 3.2.5 a and b. The agreement is again good. The last two cases taken together give the static ejected rod worth. The eigenvalues and rod worths are summarized in Table 3.2.1. The STAR rod worth is 2.0% lower than the HERMITE value.

3.2.3 Transient Results

The half core rod ejection was run with STAR using a one millisecond time step. This is the same step length as used in ARROTTA and is typical of STAR rod ejection analyses. The agreement between STAR and HERMITE is good. Figure 3.2.6 displays the core power from STAR with selected points from the reported HERMITE results. Table 3.2.2 summarizes selected results from the transient. The major difference in the results is that the peak occurs 17 milliseconds later in STAR than in HERMITE. This is probably partly due to the 2.0% lower ejected rod worth. The maximum core power differs by 2.4%, the peak power densities differ by 3.0% and the maximum fuel temperature at the end of the transient is 18°F (2.0%) lower than HERMITE.

Comparisons were made of the normalized radial power distributions from STAR and HERMITE at three times during the transient, 0.20 seconds (a point before significant heat is added and near the maximum peaking), 0.39 seconds which is near maximum power, and 0.5 seconds which is the last analyzed time in the transient. Numerical differences are shown in the comparisons rather than percent differences because of the large variation in power. Figures 3.2.7 a and b show the comparison at 0.20 seconds, Figures 3.2.8 a and b show the comparison at 0.39 seconds, and Figure 3.2.9 a and b show the comparison at 0.50 seconds. The comparisons at 0.20 seconds and 0.50 seconds, where the reactor power is insignificant or very similar between the two cases, are excellent. The agreement at 0.39 seconds is good considering that the reactor power is about 4300 Megawatts in HERMITE and about 3500 Megawatts in STAR at this time point due to the later peak in STAR.

3.2.4 Sensitivity Studies

During the development of the STAR model for the HERMITE case, a series of runs were made differing only in time step length. The core power versus time is shown in figure 3.2.10 and the maximum fuel temperature as a function of time is shown in Figure 3.2.11 for four different time steps. These figures show that the one millisecond time step is very near temporal convergence and that longer time steps give conservative results.

TABLE 3.2.1

Eigenvalue and Ejected Rod Worth Comparisons

Code	k-effective Rods In	k-effective Ejected Rod Out	Change in k-effective	$*
STAR	0.98554	0.99387	0.00833	1.142
HERMITE	0.986523	0.995033	0.008510	1.166

* Beta Effective = 0.00729634

TABLE 3.2.2

Selected Transient Results

Quantity	STAR	HERMITE
Maximum Total Core Power (MW)	4237	4339
Time of Maximum Total Core Power (s)	0.410	0.383
Peak Power Density (w/cc)	1954	2014
Time of Peak Power Density (s)	0.409	0.382
Average Fuel Temperature (°F)		
0.2 seconds	-	557
0.3 seconds	557	558
0.39 seconds (for STAR) 0.40 seconds (for HERMITE)	571	589
0.5 seconds	602	605
Maximum Fuel Temperature (°F)		
0.2 seconds	557	557
0.3 seconds	560	565
0.40 seconds	701	804
0.5 seconds	893	911

4	12 97.4	2	1	3	1	2	1 97.4	2	1	3	1	2	12 97.4	4
8	7	1	3	1	3	1	2	1	3	1	3	1	7	8
4	1 16.2	2	1	3	1 66.2	3	1	3	1 66.2	3	1	2	1 16.2	4
8	9	1	2	1	3	1	3	1	3	1	2	1	9	8
	8	2	10 97.4	2	1	3	1	3	1	2	10 97.4	2	8	
	8	11	2	1	2	1	2	1	2	1	2	11	8	
		8	8	9	1 16.2	7	12 97.4	7	1 16.2	9	8	8		
				8	4	8	4	8	4	8				

Fuel Type	k-infinity	Fuel Type	k-infinity
1	0.99579	8	1.21975
2	0.98039	9	1.06780
3	1.01849	10	1.13931
4	1.16458	11	1.08233
5	1.03258	12	0.99579

Rod insertion expressed as %-inserted from top of core.

FIGURE 3.2.1

Core Layout

LEGEND

REFERENCE
STAR
% DIFFERENCE

Y= 9									
Y= 8	1.175	1.211	1.107	.940					
	1.175	1.216	1.116	.953					
	-.01	.40	.80	1.43					
Y= 7	.983	1.219	.993	1.287	1.404	1.075			
	.982	1.218	.998	1.298	1.427	1.086			
	-.07	-.12	.46	.87	1.65	1.03			
Y= 6	.943	.858	1.005	1.019	1.269	1.392	1.075		
	.935	.855	1.000	1.024	1.280	1.416	1.086		
	-.86	-.40	-.46	.52	.89	1.75	1.03		
Y= 5	.769	.911	.827	1.058	1.413	1.269	1.404		
	.761	.899	.823	1.055	1.421	1.280	1.427		
	-1.03	-1.23	-.54	-.32	.54	.89	1.65		
Y= 4	.825	.730	.896	.852	1.058	1.019	1.287	.940	
	.811	.720	.884	.848	1.055	1.024	1.298	.953	
	-1.77	-1.38	-1.34	-.47	-.32	.52	.87	1.41	
Y= 3	.644	.771	.716	.896	.827	1.005	.993	1.107	
	.632	.755	.706	.884	.823	1.000	.998	1.115	
	-1.79	-2.06	-1.42	-1.34	-.51	-.48	.48	.71	
Y= 2	.639	.602	.771	.730	.911	.858	1.219	1.211	
	.624	.591	.756	.720	.900	.855	1.219	1.216	
	-2.41	-1.96	-2.02	-1.40	-1.21	-.40	-.04	.40	
Y= 1	.544	.639	.644	.825	.769	.943	.983	1.175	
	.532	.624	.631	.811	.760	.936	.982	1.178	
	-2.17	-2.32	-1.88	-1.73	-1.09	-.74	-.08	.25	
	9	10	11	12	13	14	15	16	17

```
EIGENVALUE - REFERENCE  =  1.00822 STANDARD DEVIATION        =   1.135
           - STAR       =  1.00695 MAX POSITIVE DIFFERENCE =   1.746
           - DIFFERENCE =  -.00127 MAX NEGATIVE DIFFERENCE =  -2.410
```

FIGURE 3.2.2

STAR-HERMITE Comparison for Static Cases 1x1 VIPRE
All Rods Out, Hot Zero Power HERMITE Reference

LEGEND

REFERENCE
STAR
% DIFFERENCE

	9	10	11	12	13	14	15	16	17
Y= 9									
Y= 8	1.108 1.109 .08	1.135 1.139 .39	1.040 1.047 .69	.881 .892 1.24					
Y= 7	.961 .961 .01	1.175 1.175 -.02	.955 .958 .27	1.190 1.195 .46	1.253 1.265 .93	.962 .967 .50			
Y= 6	.979 .974 -.50	.887 .885 -.16	1.009 1.004 -.48	.980 .980 .06	1.157 1.160 .30	1.231 1.244 1.06	.962 .967 .50		
Y= 5	.850 .847 -.42	.991 .984 -.73	.877 .874 -.34	1.057 1.051 -.56	1.320 1.318 -.14	1.157 1.160 .30	1.253 1.265 .93		
Y= 4	.955 .948 -.76	.839 .835 -.54	.993 .985 -.78	.902 .899 -.35	1.057 1.051 -.56	.980 .980 .05	1.190 1.195 .46	.881 .892 1.23	
Y= 3	.782 .779 -.37	.922 .915 -.78	.833 .829 -.49	.993 .985 -.79	.877 .875 -.32	1.009 1.004 -.48	.955 .958 .28	1.040 1.046 .60	
Y= 2	.802 .797 -.55	.748 .745 -.31	.922 .915 -.73	.839 .835 -.55	.991 .984 -.72	.887 .885 -.18	1.175 1.175 -.02	1.135 1.139 .39	
Y= 1	.694 .692 -.20	.802 .798 -.45	.782 .779 -.47	.955 .948 -.72	.850 .846 -.51	.979 .976 -.39	.961 .960 -.04	1.108 1.111 .26	

EIGENVALUE - REFERENCE = .99345 STANDARD DEVIATION = .559
- STAR = .99045 MAX POSITIVE DIFFERENCE = 1.237
- DIFFERENCE = -.00300 MAX NEGATIVE DIFFERENCE = -.785

FIGURE 3.2.3

<u>STAR-HERMITE Comparison for Static Cases 1x1 VIPRE
All Rods Out, Hot Full Power HERMITE Reference</u>

LEGEND

REFERENCE
STAR
% DIFFERENCE

	9	10	11	12	13	14	15	16	17
Y= 9									
Y= 8	.685	.994	1.231	1.205					
	.685	.999	1.250	1.230					
	.09	.41	1.54	2.12					
Y= 7	.180	.915	1.079	1.599	1.812	1.426			
	.179	.916	1.087	1.620	1.855	1.451			
	-.61	.13	.78	1.33	2.40	1.73			
Y= 6	.698	.791	1.090	1.109	1.315	1.671	1.426		
	.690	.783	1.085	1.116	1.336	1.711	1.449		
	-1.25	-.92	-.45	.65	1.63	2.39	1.59		
Y= 5	.807	.972	.872	.922	.719	1.315	1.812		
	.793	.954	.864	.919	.721	1.335	1.851		
	-1.81	-1.85	-.89	-.31	.25	1.55	2.17		
Y= 4	.914	.776	.864	.776	.922	1.109	1.599	1.205	
	.890	.759	.8[illegible]7	.766	.918	1.113	1.615	1.225	
	-2.65	-2.24	-1.[illegible]9	-1.35	-.43	.38	1.02	1.70	
Y= 3	.674	.744	.5[illegible]4	.864	.872	1.090	1.079	1.231	
	.655	.722	.500	.846	.863	1.082	1.081	1.244	
	-2.85	-2.97	-2.80	-2.09	-1.03	-.72	.22	1.05	
Y= 2	.556	.562	.744	.776	.972	.791	.915	.994	
	.536	.543	.721	.757	.951	.780	.911	.993	
	-3.47	-3.31	-3.06	-2.46	-2.15	-1.34	-.47	-.14	
Y= 1	.255	.556	.674	.914	.807	.698	.180	.685	
	.247	.536	.654	.888	.788	.685	.179	.681	
	-3.37	-3.49	-2.98	-2.89	-2.34	-1.86	-.61	-.57	

EIGENVALUE - REFERENCE = .98652 STANDARD DEVIATION = 1.745
- STAR = .98554 MAX POSITIVE DIFFERENCE = 2.396
- DIFFERENCE = -.00099 MAX NEGATIVE DIFFERENCE = -3.492

FIGURE 3.2.4

STAR-HERMITE Comparison for Static Cases 1x1 VIPRE Rodded, Hot Zero Power HERMITE Reference

LEGEND

REFERENCE
STAR
% DIFFERENCE

	1	2	3	4	5	6	7	8
Y= 9								
Y= 8						.237	.283	.293
						.240	.285	.292
						1.10	.81	-.24
Y= 7				.207	.295	.306	.251	.270
				.208	.299	.307	.251	.271
				.58	1.29	.46	.04	.15
Y= 6			.183	.231	.211	.218	.275	.273
			.185	.235	.212	.218	.273	.270
			.82	1.43	.66	-.23	-1.02	-1.21
Y= 5			.224	.174	.116	.198	.249	.385
			.228	.176	.115	.195	.246	.379
			1.47	.75	-.60	-1.31	-1.37	-1.76
Y= 4		.139	.193	.147	.152	.172	.267	.340
		.141	.194	.147	.150	.169	.261	.334
		1.15	.31	-.41	-1.25	-1.92	-2.13	-1.80
Y= 3		.141	.130	.149	.147	.190	.165	.350
		.141	.130	.147	.145	.186	.160	.341
		.28	-.54	-1.54	-1.70	[illegible]	-2.49	-2.49
Y= 2		.113	.112	.114	.170	.174	.232	.260
		.112	.111	.112	.166	.169	.226	.253
		-.80	-1.25	-1.93	-2.64	-2.65	-2.67	-2.54
Y= 1		.078	.022	.105	.144	.206	.206	.246
		.077	.022	.102	.141	.200	.201	.240
		-1.08	-1.23	-2.57	-2.77	-3.05	-2.62	-2.32

FIGURE 3.2.5 a

STAR-HERMITE Comparison for Static Cases 1x1 VIPRE
Static Ejected Worth Case, Hot Zero Power

LEGEND

REFERENCE
STAR
% DIFFERENCE

Y= 9									
Y= 8	.324	.664	.946	1.025					
	.326	.675	.970	1.061					
	.83	1.64	2.55	3.53					
Y= 7	.089	.643	.865	1.464	1.913	1.709			
	.089	.649	.880	1.493	1.968	1.740			
	.15	1.03	1.78	2.01	2.89	1.83			
Y= 6	.368	.567	.930	1.100	1.526	2.281	2.180		
	.366	.568	.934	1.113	1.556	2.329	2.199		
	-.60	.26	.40	1.20	1.93	2.10	.86		
Y= 5	.451	.725	.817	1.056	1.029	2.214	3.332		
	.447	.719	.817	1.060	1.033	2.237	3.379		
	-1.09	-.84	.05	.42	.34	1.05	1.41		
Y= 4	.551	.627	.933	1.123	1.706	2.364	3.771	3.153	
	.541	.619	.925	1.114	1.698	2.368	3.789	3.174	
	-1.80	-1.26	-.91	-.77	-.48	.18	.49	.67	
Y= 3	.445	.681	.662	1.551	1.982	3.025	3.445	4.212	
	.437	.671	.651	1.529	1.970	3.002	3.443	4.218	
	-1.86	-1.58	-1.59	-1.41	-.62	-.76	-.06	.15	
Y= 2	.403	.617	1.148	1.599	2.638	3.023	4.836	5.074	
	.393	.605	1.126	1.574	2.601	3.001	4.814	5.073	
	-2.33	-2.06	-1.93	-1.54	-1.38	-.73	-.46	-.02	
Y= 1	.195	.674	1.100	1.967	2.364	3.492	4.066	5.083	
	.191	.658	1.081	1.933	2.334	3.456	4.046	5.075	
	-2.20	-2.43	-1.72	-1.71	-1.27	-1.03	-.48	-.16	
	9	10	11	12	13	14	15	16	17

EIGENVALUE - REFERENCE = .99502 STANDARD DEVIATION = 1.455
- STAR = .99387 MAX POSITIVE DIFFERENCE = 3.532
- DIFFERENCE = -.00115 MAX NEGATIVE DIFFERENCE = -3.052

FIGURE 3.2.5 b

Static Ejected Worth Case, Hot Zero Power

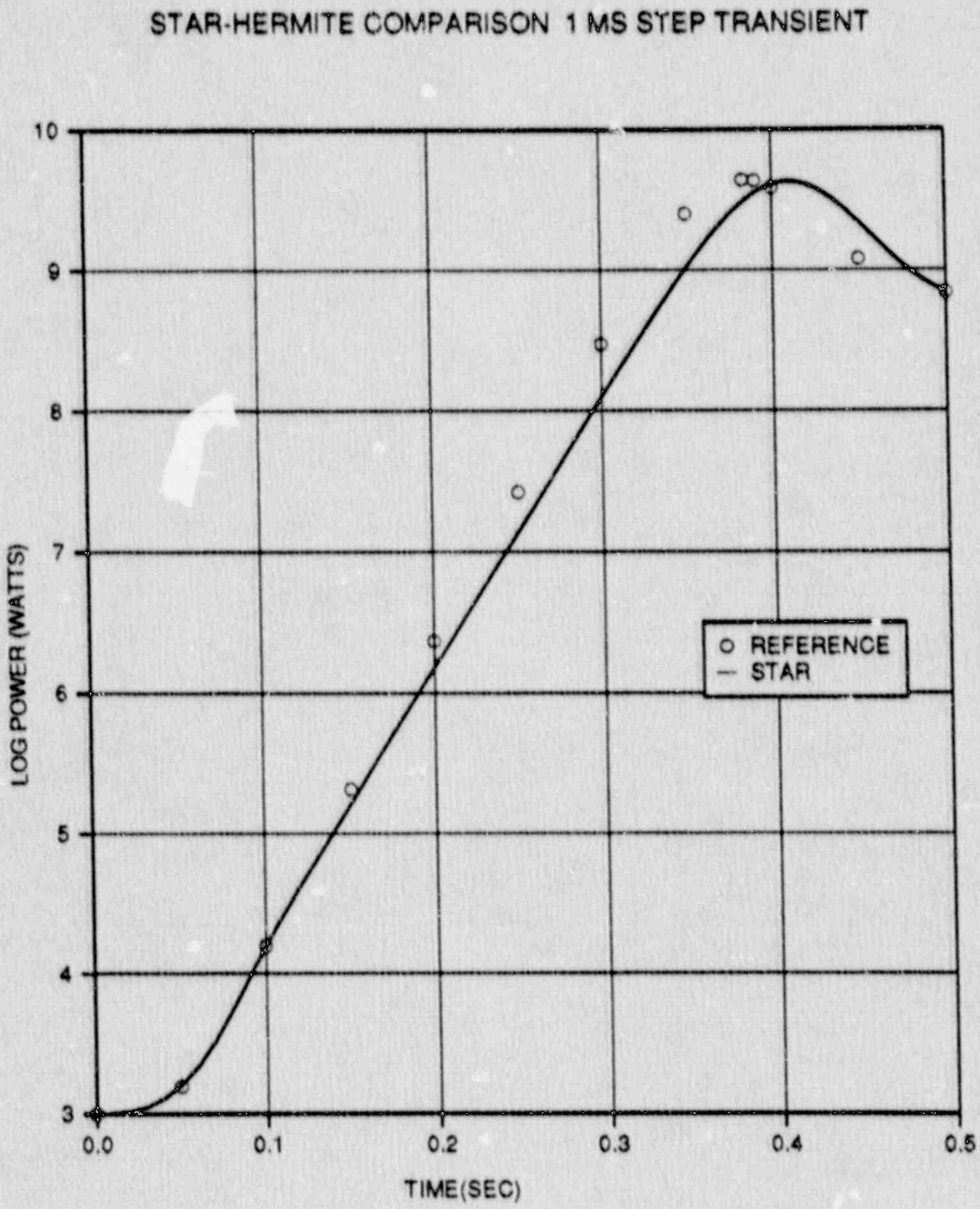

FIGURE 3.2.6

STAR - HERMITE Comparison 1 MS Step Transient

LEGEND

REFERENCE
STAR
% DIFFERENCE

	1	2	3	4	5	6	7	8
Y= 9								
Y= 8						.237	.283	.293
						.240	.285	.292
						.003	.002	-.001
Y= 7				.207	.295	.306	.250	.270
				.208	.299	.308	.251	.271
				.001	.004	.002	.000	.000
Y= 6			.184	.232	.211	.218	.275	.272
			.185	.235	.212	.218	.272	.269
			.002	.003	.002	-.000	-.003	-.003
Y= 5			.224	.175	.116	.197	.248	.384
			.228	.176	.115	.195	.245	.377
			.004	.002	-.001	-.002	-.003	-.007
Y= 4		.139	.193	.147	.151	.171	.266	.338
		.141	.194	.147	.149	.168	.260	.332
		.002	.001	-.000	-.002	-.003	-.005	-.006
Y= 3		.141	.130	.149	.146	.189	.163	.348
		.141	.129	.147	.144	.185	.159	.339
		.001	-.000	-.002	-.002	-.004	-.004	-.009
Y= 2		.113	.112	.113	.169	.172	.231	.258
		.112	.111	.111	.165	.168	.225	.252
		-.001	-.001	-.002	-.004	-.004	-.006	-.006
Y= 1		.078	.022	.105	.143	.205	.205	.244
		.077	.022	.102	.140	.199	.199	.239
		-.001	-.000	-.003	-.004	-.006	-.005	-.005

FIGURE 3.2.7 a

STAR-HERMITE Comparison 1 MS Step Transient 1x1 VIPRE Model
Assembly Power Comparison at Time = 0.2 Sec

LEGEND

REFERENCE
STAR
% DIFFERENCE

	9	10	11	12	13	14	15	16	17
Y= 9									
Y= 8	.324	.666	.948	1.031					
	.327	.677	.972	1.064					
	.003	.011	.024	.033					
Y= 7	.089	.644	.866	1.468	1.919	1.715			
	.089	.650	.881	1.497	1.974	1.746			
	.000	.007	.015	.029	.055	.031			
Y= 6	.368	.566	.931	1.101	1.531	2.289	2.187		
	.366	.568	.934	1.114	1.560	2.336	2.204		
	-.002	.002	.004	.013	.029	.047	.017		
Y= 5	.450	.723	.815	1.056	1.031	2.219	3.340		
	.445	.717	.816	1.060	1.034	2.242	3.386		
	-.005	-.006	.001	.004	.003	.023	.046		
Y= 4	.548	.624	.931	1.120	1.706	2.365	3.777	3.158	
	.538	.616	.922	1.112	1.697	2.368	3.795	3.178	
	-.010	-.008	-.008	-.008	-.008	.003	.018	.020	
Y= 3	.443	.678	.659	1.547	1.978	3.024	3.447	4.218	
	.435	.668	.649	1.525	1.966	3.001	3.444	4.223	
	-.008	-.011	-.010	-.022	-.012	-.023	-.003	.006	
Y= 2	.401	.614	1.143	1.591	2.632	3.020	4.840	5.081	
	.392	.602	1.122	1.569	2.595	2.998	4.818	5.078	
	-.009	-.012	-.021	-.022	-.037	-.022	-.022	-.003	
Y= 1	.194	.671	1.095	1.960	2.358	3.489	4.066	5.089	
	.190	.655	1.076	1.927	2.328	3.453	4.046	5.079	
	-.004	-.016	-.019	-.033	-.030	-.036	-.020	-.010	

STANDARD DEVIATION = .015
MAX POSITIVE DIFFERENCE = .055
MAX NEGATIVE DIFFERENCE = -.037

FIGURE 3.2.7 b

Assembly Power Comparison at Time = 0.2 Sec

LEGEND

REFERENCE
STAR
% DIFFERENCE

	1	2	3	4	5	6	7	8
Y= 9								
Y= 8						.276 .259 -.017	.324 .306 -.018	.327 .309 -.018
Y= 7				.250 .229 -.021	.351 .326 -.024	.357 .333 -.025	.286 .268 -.018	.302 .286 -.015
Y= 6			.224 .205 -.020	.281 .259 -.022	.251 .232 -.019	.254 .235 -.019	.312 .290 -.022	.301 .283 -.018
Y= 5			.276 .253 -.023	.213 .194 -.018	.138 .126 -.012	.228 .209 -.018	.278 .259 -.019	.419 .394 -.025
Y= 4		.173 .157 -.016	.238 .215 -.023	.179 .162 -.017	.180 .163 -.017	.197 .180 -.017	.296 .275 -.021	.367 .346 -.021
Y= 3		.175 .158 -.017	.160 .144 -.017	.181 .162 -.019	.174 .157 -.017	.218 .199 -.019	.182 .168 -.014	.375 .352 -.023
Y= 2		.141 .125 -.015	.138 .123 -.015	.137 .122 -.015	.200 .179 -.021	.199 .180 -.018	.257 .237 -.020	.279 .262 -.017
Y= 1		.096 .086 -.011	.028 .025 -.003	.126 .112 -.014	.169 .152 -.018	.236 .213 -.022	.229 .211 -.018	.264 .248 -.016

FIGURE 3.2.8 a

STAR-HERMITE Comparison 1 MS Step Transient 1x1 VIPRE Model
Assembly Power Comparison at Time = 0.39 Sec

LEGEND

REFERENCE
STAR
% DIFFERENCE

	9	10	11	12	13	14	15	16	17
Y= 9									
Y= 8	.348	.698	.983	1.060					
	.339	.693	.991	1.079					
	-.009	-.004	.008	.019					
Y= 7	.095	.672	.896	1.499	1.936	1.713			
	.092	.665	.897	1.514	1.984	1.746			
	-.003	-.007	.001	.015	.048	.033			
Y= 6	.392	.592	.959	1.120	1.535	2.266	2.150		
	.378	.581	.949	1.125	1.563	2.326	2.187		
	-.014	-.011	-.010	.005	.028	.060	.037		
Y= 5	.479	.755	.837	1.066	1.023	2.174	3.252		
	.460	.733	.827	1.066	1.031	2.220	3.343		
	-.019	-.021	-.010	.000	.008	.046	.091		
Y= 4	.581	.649	.948	1.120	1.676	2.299	3.643	3.036	
	.555	.629	.932	1.113	1.684	2.336	3.728	3.117	
	-.026	-.019	-.016	-.007	.008	.037	.085	.081	
Y= 3	.466	.700	.666	1.533	1.935	2.923	3.304	4.029	
	.447	.679	.653	1.519	1.946	2.951	3.372	4.128	
	-.020	-.021	-.013	-.014	.011	.028	.068	.099	
Y= 2	.419	.627	1.146	1.571	2.565	2.910	4.618	4.832	
	.401	.609	1.124	1.561	2.563	2.944	4.706	4.952	
	-.018	-.018	-.022	-.010	-.002	.034	.088	.120	
Y= 1	.202	.682	1.095	1.933	2.296	3.357	3.898	4.836	
	.194	.661	1.077	1.915	2.299	3.387	3.952	4.950	
	-.008	-.021	-.018	-.018	.003	.030	.054	.114	

STANDARD DEVIATION = .033
MAX POSITIVE DIFFERENCE = .120
MAX NEGATIVE DIFFERENCE = -.026

FIGURE 3.2.8 b

<u>Assembly Power Comparison at Time = 0.39 Sec</u>

LEGEND

REFERENCE
STAR
% DIFFERENCE

	1	2	3	4	5	6	7	8
Y= 9								
Y= 8						.330 .332 .002	.379 .381 .001	.371 .369 -.002
Y= 7				.311 .311 .000	.430 .433 .003	.428 .428 -.000	.335 .334 -.001	.343 .341 -.001
Y= 6			.284 .285 .000	.352 .354 .003	.308 .308 .000	.303 .301 -.002	.361 .356 -.005	.336 .331 -.005
Y= 5			.351 .354 .002	.268 .268 .000	.169 .167 -.002	.269 .264 -.005	.319 .313 -.006	.463 .454 -.010
Y= 4		.223 .223 .001	.305 .304 -.001	.226 .224 -.002	.220 .216 -.004	.232 .227 -.006	.336 .328 -.008	.402 .393 -.008
Y= 3		.226 .225 -.001	.206 .203 -.003	.228 .223 -.005	.212 .207 -.005	.257 .250 -.007	.206 .200 -.006	.409 .398 -.011
Y= 2		.182 .179 -.003	.176 .173 -.003	.171 .167 -.005	.243 .235 -.008	.234 .227 -.007	.292 .283 -.009	.304 .296 -.009
Y= 1		.125 .122 -.002	.035 .034 -.001	.156 .151 -.005	.205 .199 -.007	.277 .268 -.010	.260 .252 -.008	.289 .281 -.008

FIGURE 3.2.9 a

STAR-HERMITE Comparison 1 MS Step Transient 1x1 VIPRE Model
Assembly Power Comparison at Time = 0.5 Sec

LEGEND

REFERENCE STAR % DIFFERENCE

	9	10	11	12	13	14	15	16	17
Y= 9									
Y= 8	.376	.733	1.020	1.088					
	.378	.742	1.043	1.120					
	.002	.010	.023	.032					
Y= 7	.103	.704	.926	1.527	1.944	1.701			
	.102	.709	.940	1.556	1.997	1.732			
	-.000	.005	.014	.029	.053	.031			
Y= 6	.422	.620	.988	1.136	1.531	2.226	2.096		
	.418	.620	.990	1.149	1.561	2.275	2.117		
	-.004	.000	.002	.013	.030	.049	.022		
Y= 5	.513	.789	.858	1.074	1.010	2.111	3.132		
	.506	.781	.858	1.077	1.013	2.137	3.182		
	-.007	-.008	-.001	.003	.003	.026	.050		
Y= 4	.620	.675	.964	1.114	1.637	2.214	3.472	2.881	
	.607	.666	.955	1.107	1.631	2.222	3.497	2.908	
	-.013	-.009	-.009	-.008	-.006	.008	.025	.027	
Y= 3	.494	.723	.672	1.511	1.878	2.796	3.126	3.793	
	.484	.710	.662	1.491	1.869	2.780	3.132	3.809	
	-.010	-.012	-.010	-.020	-.009	-.016	.006	.016	
Y= 2	.441	.640	1.145	1.542	2.478	2.773	4.345	4.524	
	.430	.627	1.124	1.522	2.447	2.759	4.337	4.534	
	-.011	-.014	-.021	-.020	-.031	-.014	-.008	.010	
Y= 1	.212	.692	1.091	1.894	2.217	3.194	3.650	4.523	
	.207	.675	1.073	1.863	2.192	3.167	3.641	4.526	
	-.005	-.017	-.018	-.031	-.025	-.027	-.009	.003	

STANDARD DEVIATION = .015
MAX POSITIVE DIFFERENCE = .053
MAX NEGATIVE DIFFERENCE = -.031

FIGURE 3.2.9 b

Assembly Power Comparison at Time = 0.5 Sec

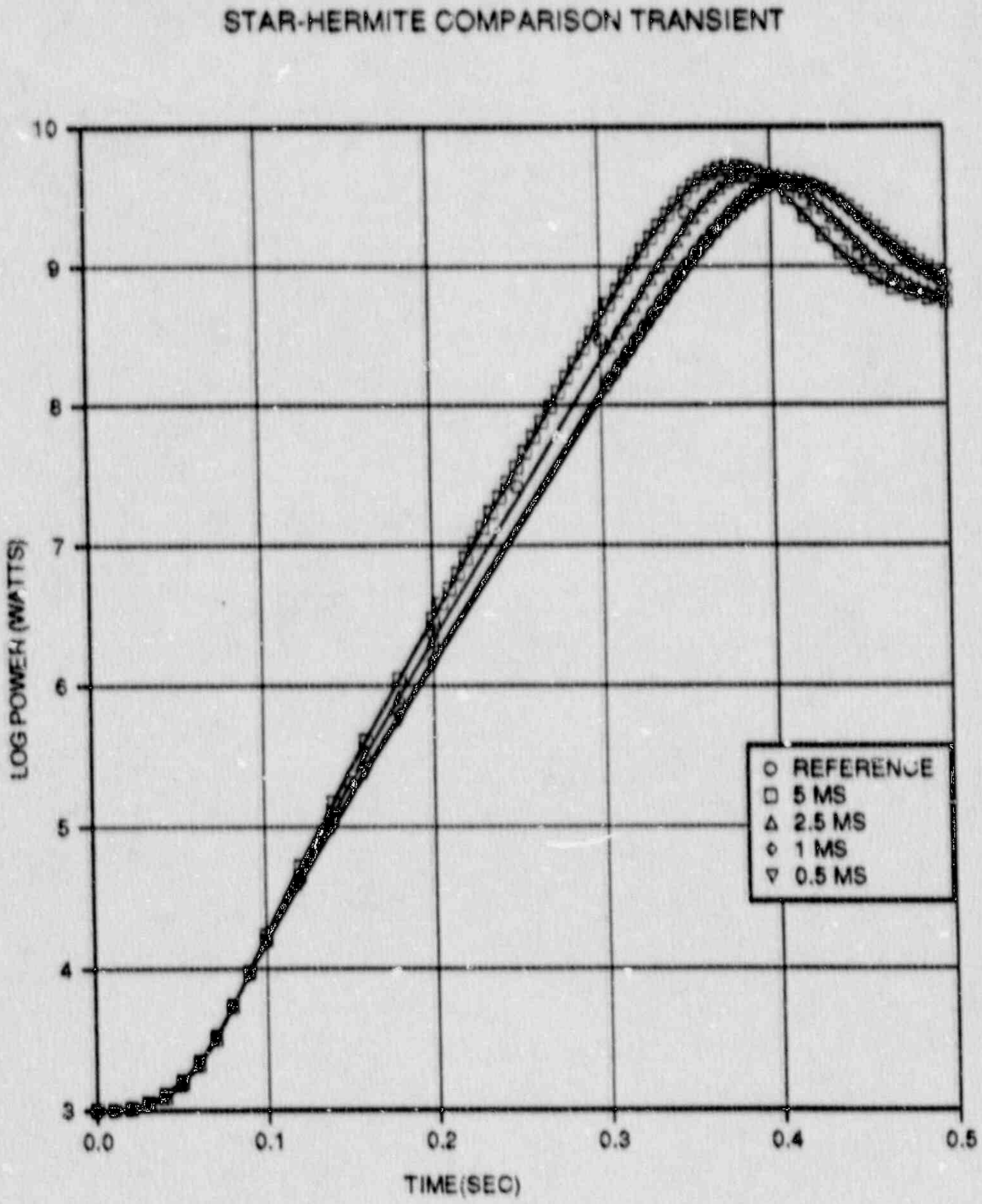

FIGURE 3.2.10

STAR - HERMITE Comparison Transient

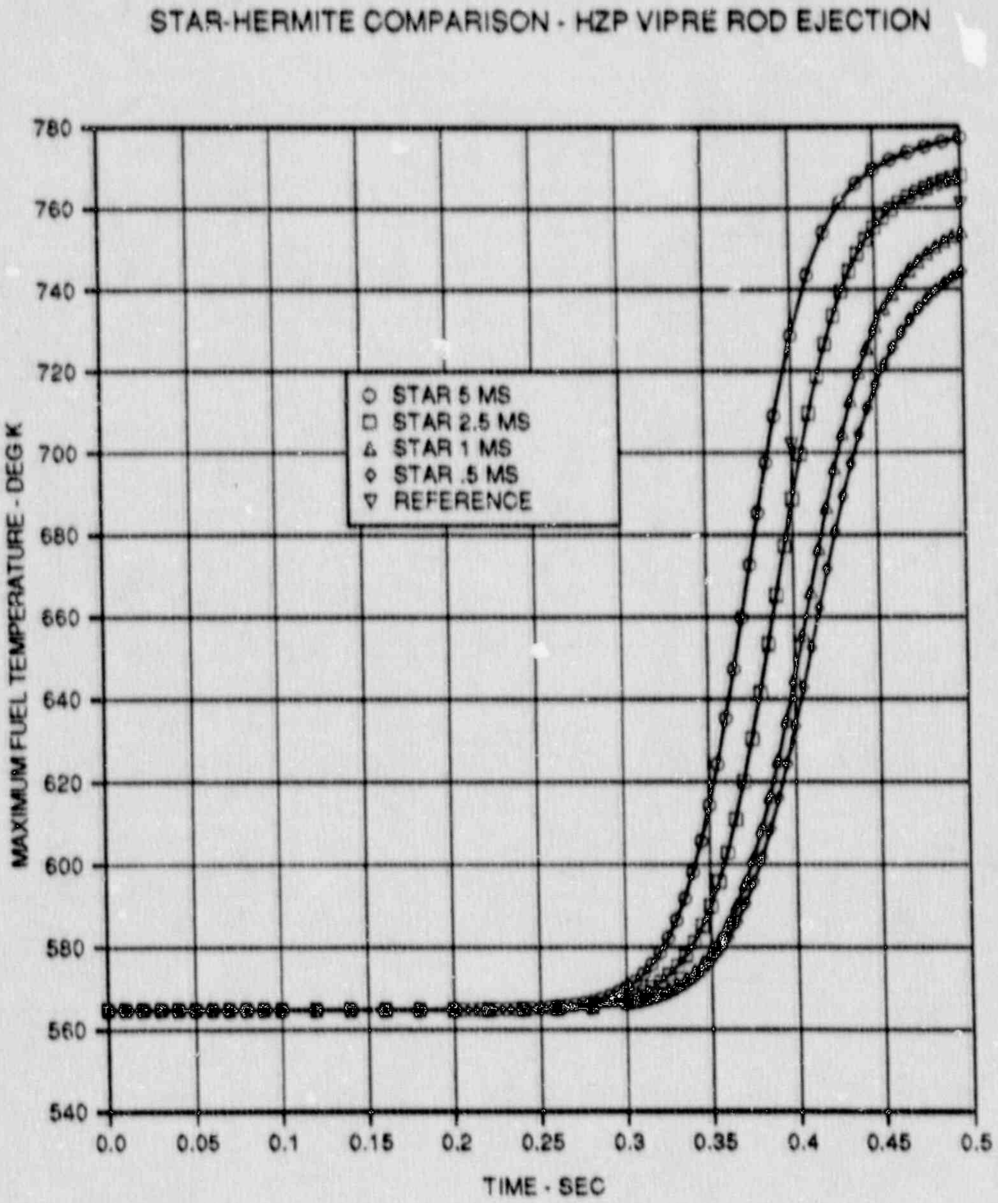

FIGURE 3.2.11

STAR - HERMITE Comparison - HZP VIPRE Rod Ejection

3.3 Yankee Rowe Rod Drop

At approximately 12:02 AM on February 18, 1987, near the end of Cycle XVIII, a high worth group A control rod dropped into the Rowe core during full power operation. This rod was worth about 0.47% $\Delta\rho$, and is one of a group of 4 near the center of the core. This event did not cause an immediate plant trip.

The first 16 seconds of this event were modeled using the STAR code with 4 radial nodes per assembly, 12 axial nodes, SIMULATE-3 cross sections, and the VIPRE-01 thermal hydraulic option. Comparisons have been made with excore detector data (mostly at 4 second intervals) and core exit thermocouples at 8 second intervals assuming the drop took place at 00:02:04 exactly and that the rod drop time was 1.6 seconds.

Figure 3.3.1 shows the STAR calculated core power compared to the excore detectors. Channel 6 is the nearest detector to the dropped rod. The shape and magnitude of the STAR power are in good agreement with the measurements, considering that the dropped rod is near the center of the core and that the excore detectors are reading the power of the outer part of the core.

Figures 3.3.2 and 3.3.3 compare the measured and STAR predicted outlet thermocouple temperatures at the time of the drop, and the measured and predicted temperature change for each thermocouple that responded to the transient. Figure 3.3.2 shows that the STAR and measured distributions agree well with the STAR mean being somewhat lower. Figure 3.3.3 shows that the predicted and measured changes during the transient also agree well in magnitude and in spatial distribution with the STAR predicted mean change being somewhat higher. The dropped rod location is surrounded by locations F5, F6, G5 and G6.

This analysis shows that STAR can analyze operational events with good accuracy if data is available at reasonable time intervals.

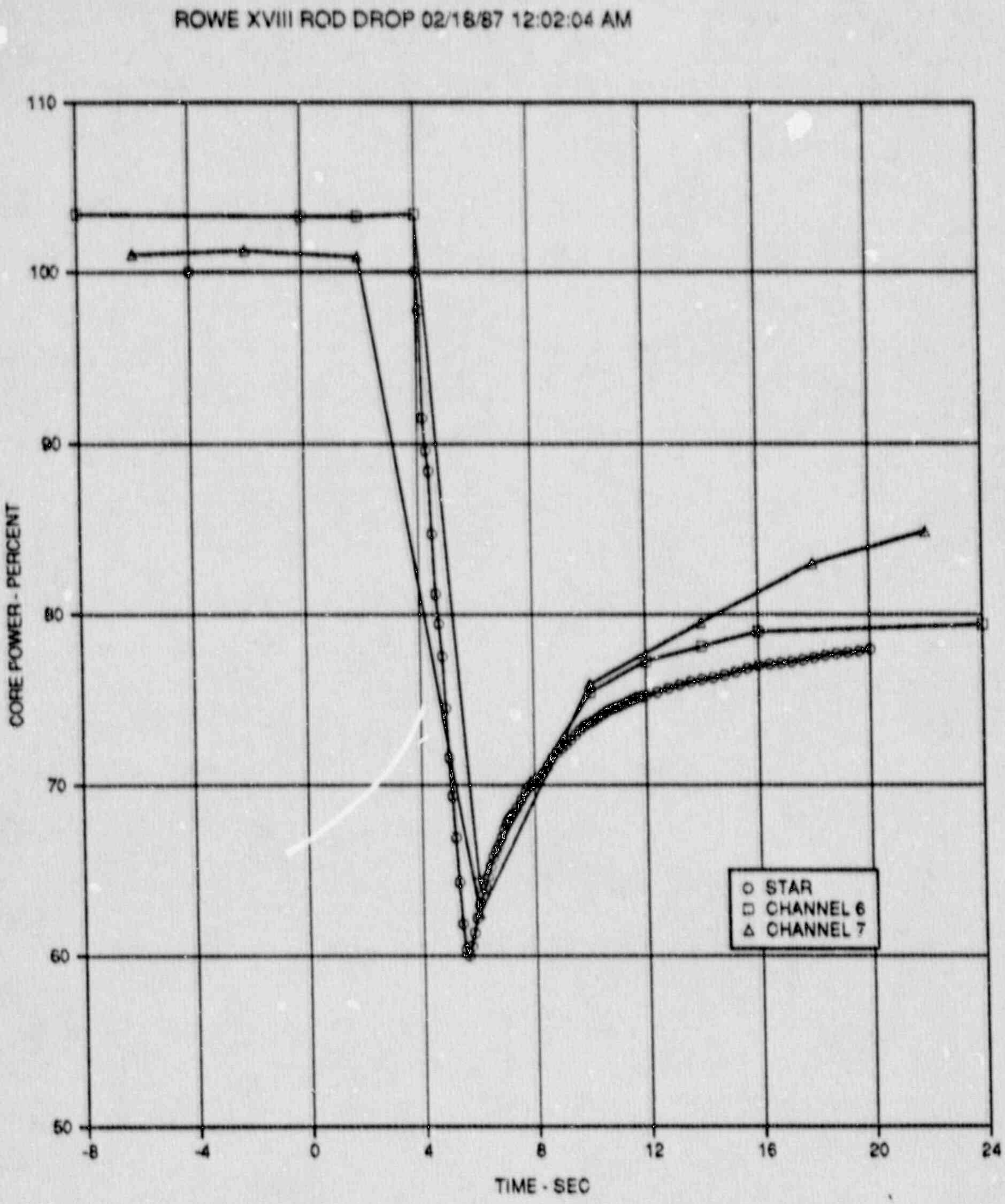

FIGURE 3.3.1

Rowe XVIII Rod Drop 02/18/87 12:02:04 AM

	A	B	C	D	E	F	G	H	J	K
1				D1 549.71 540.95	E1 551.60 548.60					
2			C2 550.71 546.75	D2 563.48 561.24						
3		B3 550.21 546.62		D3 562.39 562.73						
4			C4 556.00 559.85		E4 566.57 564.80					
5	A5 551.24 548.60		C5 561.40 559.31		E5 561.38 561.47			H5 563.31 561.33		
6										
7		B7 571.97 560.93				F7 567.09 564.62		H7 560.30 560.03		
8										
9										
10							G10 543.41 541.26			

CET Mean Temperature = 558.17 °F
STAR Mean Temperature = 555.57 °F

Bad CET's D4, D5, D8 Rejected

INITIAL TEMPERATURES

CET	°F
STAR	°F

FIGURE 3.3.2

2/18/87 Rowe Rod Drop Core Exit Thermocouple Analysis

	A	B	C	D	E	F	G	H	J	K
1				D1 6.29 7.06	E1 6.29 6.77					
2			C2 7.18 7.67	D2 7.19 10.62						
3		B3 7.18 7.38		D3 8.09 11.34						
4			C4 6.29 10.08		E4 12.58 14.90					
5	A5 8.09 7.34		C5 8.99 10.17		E5 13.48 16.25			H5 15.27 18.59		
6										
7		B7 10.79 9.45				F7 14.37 17.73		H7 7.19 15.97		
8										
9										
10							G10 8.09 8.23			

CET Mean Temperature Change = 9.21 °F
STAR Mean Temperature Change = 11.36 °F

Bad CET's D4, D5, D8 Rejected

TEMPERATURE CHANGE

CET	°F
STAR	°F

FIGURE 3.3.3

2/18/87 Rowe Rod Drop Core Exit Thermocouple Analysis

4.0 SUMMARY AND CONCLUSIONS

Volume 1 of this report has provided a discussion of the theory of the STAR computer code. A significant amount of benchmark material was also provided, covering classical numerical problems, a vendor code comparison, and a comparison to an actual plant transient.

The results of the classical numerical benchmarks show excellent agreement with the reference results. The comparison to Combustion Engineering's HERMITE computer code, which STAR will replace in our current rod ejection method, demonstrates good agreement between the two codes. The benchmark of the Rowe rod drop transient shows that STAR compares well to actual plant transient data. Overall the benchmark work provided in this volume demonstrates that STAR is a valid code to use in our methods which require a three dimensional space time reactor physics code.

5.0 REFERENCES

1. WAPD-TM-479, "CHIC-KIN - A FORTRAN Program for Intermediate and Fast Transients in a Water Moderated Reactor," J. A. Redfield, January, 1965.

2. YAEC-1464, "Modified Method for CEA Ejection Analysis of Maine Yankee Plant," December, 1984.

3. CENPD-190-A, "CE Method for Control Element Assembly Ejection Analysis," January, 1976.

4. USNRC Memorandum to G. C. Lainas from L. S. Rubenstein, "Safety Evaluation Report of YAEC-1464 Maine Yankee Modified Method for CEA Ejection Analysis," June 20, 1985.

5. YAEC-1398, "Yankee Nuclear Power Station Main Steam Line Break Analysis Addition of Boron Transport Model," February, 1984.

6. YAEC-1447, "Application of RETRAN-02 MOD 02 and BIRP to the Analysis of the MSLB Accident at MYAPC," September, 1984.

7. NMY 85-166, "Safety Evaluation of the Maine Yankee Atomic Power Corporation (MYAPC) Report YAEC-1447, Applications of RETRAN-02 MOD 02 and BIRP to the Analysis of the MSLB Accident at MYAPC," E. J. Butcher, October 2, 1985.

8. Joint EPRI Publication - MIT Nuclear Engineer Thesis,"An Analytic Nodal for Solving the Two-Group, Multidimensional Static and Transient Neutron Diffusion Equation," K. Smith and A. F. Henry, March, 1979.

9. Report to EPRI, "Recent Advances in an Analytic Nodal Method for Static and Transient Reactor Analysis," K. Smith, G. Greenman, A. F. Henry, June, 1979.

10. Transactions ANS, 47 pages 411 - 412, "Accurate Solution of the Transient Three Dimensional CMFD Diffusion Equations," C. L. Hoxie, A. Wertzberg, and W Herwig, 1984.

11. Proceedings from the International Meeting on Advances in Nuclear Engineering Computational Methods, Vol. 2, "A Nonlinear Coupling Coefficient Iteration for Solving the Nodal Three Dimensional Diffusion Equation," C. L. Hoxie, 1985.

12. ORNL-TM-2496, "Nuclear Reactor Core Analysis Code: CITATION," Oak Ridge National Laboratory, T. B. Fowler, D. R. Vondy, and G. W. Cunningham, 1971.

13. Transactions ANS, 22 page 250, "Higher Order Corrections in Nodal Reactor Calculations," F. Bennewitz, H. Finnemann, and M. R. Wagner, 1975.

14. MIT PHD Thesis, "Spatial Homogenization Methods for Light Water Reactors", K. S. Smith, 1980.

15. Paper Presented at the IAEA Technical Committee Meeting on Homogenization Methods in Reactor Physics, "A New Approach to Homogeneous and Group Condensation," K. Koebke, November, 1978.

16. STUDSVIK/SOA-89/03, "SIMULATE-3 Advanced Three-Dimensional Two-Group Reactor Analysis Code," Users Manual Version 3.0, November, 1989.

17. Prentice-Hall Englewood Cliffs, NJ, "Iterative Solution of Elliptic Systems and Applications to the Neutron Diffusion Equations of Reactor Physics," 1966.

18. Transactions ANS, Vol 44, pages 265 - 266, "Nodal Method Storage Reduction by Nonlinear Iteration," K. S. Smith, 1983.

19. Prentice-Hall Englewood Cliffs, NJ, "Matrix Iterative Analysis," R. Varga,

20. WAPD-TM-788, "WIGL-3 a Program for the Steady-State and Transient Solution of the One-Dimensional Two-Group, Space-Time Diffusion Equations Accounting for Temperature, Xenon, and Control Feedback," A. V. Vota, N. J. Curlee, Jr., A. F. Henry, February, 1969.

21. ANL-7416 Supplement 2, "Argonne Code Center: Benchmark Problem Book," 1977.

22. BNWL-1695, "COBRA-IIIC a Digital Computer Program for Steady-State and Transient Thermal Hydraulic Analysis of Rod Bundle Nuclear Fuel Elements," D. S. Rowe, March, 1973.

23. EPRI-NP-2511-CCM, "VIPRE-01: A Thermal Hydraulic Analysis Code for Reactor Cores," 4 volumes, Electric Power Research Institute, April 1983, Rev. 1, November 1983, Rev. 2, July 1985.

24. Nuclear Science and Engineering 38, 8, "Comparison of Alternating-Direction Time-Differencing Methods and Other Implicit Methods for the Solution of the Neutron Group Diffusion Equation," L. A. Hageman and J. B. Yasinsky, 1969.

25. Nuclear Science and Engineering 63, 437-456, "Coarse Mesh Nodal Diffusion Method for the Analysis of Space Time Effects in Large Light Water Reactors," S. Lagenbush, W. Maurer, and W. Werner, 1977.

26. Electric Power Research Institute, "ARROTTA: Advanced Rapid Reactor Operational Transient Analysis Computer Code Documentation Package," Volume 1: Theory and Numerical Analysis, and Volume 2: User's Manual, L. D. Eisenhart, February, 1989.

27. CENPD-188-A, "HERMITE: A Multi-dimensional Space-Time Code for PWR Transients," Combustion Engineering, Inc., P. E. Rohan, S. G. Wagner, S. E. Ritterbusch, July, 1976.

28. EPRI NP-6614, "ARROTTA - HERMITE Code Comparison," Electric Power Research Institute, P. E. Rohan, S. G. Wagner, December 1989.